

Response: second round

Editor's comments

Thanks for submitting your revised manuscript. In reviewing your responses, especially reviewer #4, you have provided strong rebuttals to the reviewer, however, you have not made any substantial changes to the manuscript to clarify the various points raised by the reviewer. I ask that you and your co-authors please re-consider All the reviewer comments (not just RC4), and make sure enough changes are made to the manuscript to clarify the criticisms made the reviewers, rather than only address this in your reply. This will help future readers of the manuscript who may have similar questions. For example, i would expect to see a few sentences in your introduction, which explains how your work further builds on the Rayner, Knorr and Wang papers, as per your rebuttal.

Response:

We thank the editor for his comment and acknowledge that the changes we have made to the text could have been slightly more substantial to highlight the issues raised the 4 reviewers. We thus report below the 4 reviews with our initial responses and describe for each comment any new additional changes we have made to the main text (when relevant). We hope that with these additional revisions ensure that all concerns raised initially by the reviewers are properly discussed in the manuscript.

Note that in our rebuttal to the comments of reviewer 4, we made a little mistake when citing Wang paper as it should have been Knorr and Heimann (1995). Wang et al. (2001) was already cited when describing studies that have assimilated in situ FluxNet data.

Response to reviewer 1

Peylin and colleagues describe a Carbon Cycle Data Assimilation System based on the land-surface model ORCHIDEE optimized against NDVI data, eddy covariance CO₂ flux data, and atmospheric CO₂ data. For practical reasons, these three data streams are used successively in three steps. The paper describes the system, assesses its performance (especially the self-consistency across the three steps), and some features of the resulting carbon cycle fluxes and stocks. The authors conclude that the ORCHIDEE land-surface model is now structurally adequate enough to bridge the information from the three data streams, though they also highlight further steps that need to be taken to represent the global carbon cycle more accurately.

The study represents an interesting and relevant development in the understanding of the carbon cycle consistent with available data. There are open issues (for example the short assimilation period precluding various processes to be constrained and assessed) but these are clearly acknowledged in the paper. I find the presentation clear and convincing. In my opinion, the work should be published in Geoscientific Model Development.

First response:

We thank the reviewer for his positive appreciation of the manuscript.

Minor comments:

p 5 l 6: The associativity is true for linear systems, but is it really also true for nonlinear systems? (I nevertheless agree to the arguments given in favor of the step-wise approach.)

First response:

The associativity argument, detailed in Tarantola (2005), relies on the combination of probability density functions (PDFs) through the Bayes theorem without any assumption on the linearity or non-linearity of the system. It is a general property associated to the combination of probability distribution (i.e., the description of the probability of an event, based on conditions that might be related to that event). So the non-linearity does not invalidate the step-wise approach; it only highly complicates the computation of the full PDFs at each step and thus their propagation. The necessary simplifications that are made in this case lead to the complication investigated in the paper. In the case of a linear system, we could have easily calculated and propagated the full PDFs.

We have completed one sentence in the introduction to reinforce that the associativity does not depend on the linearity of the system:

“This multiplication is associative so it makes no differences whether it is performed in one step or several (and whether the system is linear or not).”

Second response:

No addition to the previous modification as we already added one sentence into the manuscript as detailed above.

p 8 l 13: What is the uncertainty due to incomplete sampling of the diurnal cycle?

First response:

We have not estimated the uncertainty due to a possible 20% gap. However, in order to compute the daily mean values, we have used gap-filled data so that the uncertainty only arises due to errors in the gap-filling procedure. Such uncertainty, usually less than 20 % (Lasslop et al. 2008), would thus only affect 20% at maximum of the diurnal cycle; it would thus have an overall negligible impact compared to the model uncertainty that need to be also accounted for.

Second response:

We completed the text with the following sentence: “Note that uncertainties due to incomplete sampling of the diurnal cycle are likely very small (less than 5%) as the error in the gap-filling procedure is usually less than 20% (Lasslop et al., 2008).”

p 14 l 25-26: I was wondering whether the presence of step functions, creating discontinuities, still allows a well-defined solution of the minimization?

First response:

We agree that step functions may complicate the minimization problem, creating potentially non-smooth cost function, i.e. with a “singular” point where the derivative is not defined and not continuous. However the use of finite differences to compute the gradient for these

parameters allows defining a “mean derivative” at any point (mean as for non local). As a result the iterative approach (BFGS algorithm) used to search for the minimum may oscillate if we end up for a given parameter in the vicinity of the discontinuity, but it will not diverge. However such situation is very unlikely to occur and we have checked that no obvious oscillation for each parameter was occurring.

We completed one sentence in the text to precise this point:

“A finite difference approach was used for these parameters in order to define a mean derivative at any point”.

Second response:

We completed the added sentence: “A finite difference approach was used for these parameters in order to define a mean derivative at any point; we also checked that no spurious oscillations occurred for these parameters during the minimization iterations.”

p 17 l 25-30: Add references for "University of Stuttgart" and "ENSTO-E". Explain abbreviation "IER".

First response:

We now explain the “IER” abbreviation and we provide two web references for both "University of Stuttgart" and "ENSTO-E".

Second response:

No addition

p 20 l 14: What does "conditions" mean here?

First response:

We have changed the text to precise that “conditions” was referring to station sampling air “representative of different geographical regions of influence”.

Second response:

No addition

p 21 l 4: Clarify whether this is the prior before step 1 or before step 3?

First response:

It is the prior of step 3 and we have now clarified the text.

Second response:

No addition

p 22 l 21: Can you give just a brief summary of the reasons here?

First response:

We have improved the text to provide a brief summary of these reasons:

- The NDVI or fAPAR mainly constrain the timing of the ecosystem GPP and only to a small extent the amplitude of the GPP, given that the satellite signal is likely

- to saturate during the peak of the growing season.
- The NDVI or fAPAR do not constrain the ecosystem respiration at all, which is an important component of the NEE, at least at seasonal to annual scales.

Second response:

We only slightly change the first reason as: “The NDVI or fAPAR mainly constrain the timing of the leaf phenology (and thus indirectly the GPP) and “

p 25 l 24: These are clearly not the numbers shown in Fig 10 right.

First response:

We apologize for such mistake as the numbers correspond indeed from a previous experiment.

We have corrected the text with the exact numbers from figure 10b.

Note that the exact numbers from figure 10b do not change the overall message and the rather small reduction of the GPP from the prior to the posterior of step 3.

Second response:

No addition

p 27 l 6: Can you explain (here or earlier) why you used individual grid points rather than the whole grid?

First response:

The main reasons for choosing only a set of individual grid points are twofold:

- First, we proposed to use only the model grid point that are covered by a vegetation fraction greater than 60% for a given PFT, avoiding the use of grid points with a large mix of PFTs so that the optimization of the phenological parameters for each PFT is more straightforward. This is explained in section 2.4.1 (step 1).
- We then limited the selected set of points to 15 in order to significantly reduce the computing time of the step 1 optimization. Doing so further allows evaluating the optimized model at all pixels that were not used for the optimization.

We added a sentence in section 2.4.1 (step 1 paragraph) to better explain our choice:

“Only grid cells that included vegetation fraction of greater than 60% for the PFT optimized were considered. We selected a set of grid points instead of the whole grid to substantially decrease the computing time; but the remaining points are used for the evaluation of the optimized model.”

Second response:

No addition

p 29 l 10: I think you should also mention the errors in the prescribed fossil fuel and ocean fluxes.

First response:

We added at the end of the paragraph a sentence to mention the importance of the errors associated to the prescribed fossil fuel and ocean fluxes:
“Additionally, uncertainties on the other components of the carbon cycle, such as fossil fuel and biomass burning emissions and ocean fluxes, can be also critical when using atmospheric CO₂ as a constraint.”

Second response:
No addition

Fig 5: I don't see any grey lines.

First response:
We have corrected the caption as we do not included the “prior of step 1” in this version of the figure in order not to overload the figure with too many curves.

Second response:
No addition

Response to reviewer 2

Peylin et al. contribute an interesting study on the effect of using a stepwise optimisation rather than merging all data streams in a single cost function. This is a procedure that we have used in e.g. catchment scale water quality modelling where one first calibrates the water cycle before calibrating parameters relevant to nutrient diffusion (e.g. Exbrayat et al., 2011). However, this approach has not been investigated in details in the frame of the (global) carbon cycle. Therefore, I agree with reviewer #1 that this paper is highly relevant to the community. I particularly like the several steps used by the authors to reconcile site-scale calibration with global atmospheric concentrations.

I have some very minor comments on the paper that should be straightforward to address:

First response:
We thank the reviewer for his positive evaluation of the paper.

p.5 l.1: another alternative to stepwise optimisation and simultaneous procedure is a simultaneous, multi-objective approach based on the Pareto ranking of several cost functions to account for trade-offs (e.g. Yapo et al., 1998). Would it be realistic to use such an approach in this system to avoid the increase in RMSE against MODIS NDVI from step1 to step2 (fig. 8, TeBD)?

First response:
The suggestion of using a simultaneous multi-objective approach based on the Pareto ranking of several cost functions to account for trade-offs as in Yapo et al. (1998) could indeed appear as an alternative approach. However, it is based on a random generation of parameter sets in order to find the so-called “Pareto parameter space” where all parameter sets lead to equal overall objective function but with trade-offs between individual cost functions. With the global carbon cycle optimization problem and the ORCHIDEE model the approach in Yapo et al. (1998) is from a computational point of view not feasible at all. For a specific hydrology

problem with 13 parameters to be optimized and two cost functions the proposed algorithm required more than 68000 function evaluations to converge to a solution. Given that our total number of parameters is on the order of 100 and that we can not afford a large number of global simulation for the evaluation of the cost function linked to atmospheric CO2 data (few tens to a hundred), such method is thus clearly not suitable.

Finally we should mention that the increase in RMSE against MODIS NDVI from step1 to step2 is relatively small compared to the initial improvement of the RMSE during step1 optimization.

Second response:

We have included in the introduction a new sentence to mention that such alternatives are not affordable: “Note finally that more complex approaches based on random generation of parameter sets, such as the multi-objective approach using the Pareto ranking of several cost functions (e.g. Yapo et al., 1998), are not yet affordable for global LSMs from a computational point of view.”

p.5 l.12-13: Using a restricted number of parameters is a valid point but it needs to be mentioned here that one must proceed to some sort of sensitivity analysis to accurately select these parameters.

First response:

We agree that the selection of parameters should follow a rigorous sensitivity analysis, using for example the MORRIS algorithm (global sensitivity analysis; Morris, 1991). In our case, we have done such sensitivity analysis in previous studies with the ORCHIDEE model; we have thus kept the same set of parameters that was identified in these studies. We have improved the text adding: “(following a global sensitivity analysis)”.

Second response:

No addition

p.8 l.1: why not using only days with data?

First response:

We agree with the reviewer that we could have used only the days with data. However, for practical implementation it was easier to interpolate the time series that have sparse data. We have checked however that using this interpolation does not change the results of the optimization.

Second response:

We completed the text adding that such choice was made for “practical implementation”

p.9 l.26: please mention the resolution of the model here

First response:

We added the resolution of the LMDz model.

Second response:

No addition

p. 10 l.1: is it robust to assume that carbon pools are at equilibrium in 1990? Could this system use a prior from soil and biomass maps instead (like e.g. Bloom et al., 2016)?

First response:

The choice to bring the model at equilibrium for the carbon pools in 1990 is a compromise. We do not think that our optimization system could easily use soil map (such as the HWSD data set) or forest biomass estimates (such as the Saatchi et al (2011) map for the Tropics).

For the soil carbon content, it is not straightforward to use the HWSD map to force a global model like ORCHIDEE. First, with the “CENTURY” soil carbon model used in ORCHIDEE, the turn over time of the soil organic matter (for each reservoirs) together with the rate of organic matter input to the soil (litter and root turnover) determine a total soil carbon content that is in balance with all components of the model. It is thus difficult to optimize the soil carbon content with global estimates such as HWSD, while keeping the internal model consistency. One way would be to optimize the parameters controlling the turnover times as well as the soil carbon input over a long spin up period (several 1000 years); this is currently not feasible with the optimization of several parameters, especially without the adjoint of the model. Second the model does not represent yet high soil carbon content such as peat land or permafrost, while these soil type are usually taken into account in the observations. Finally, the HWSD soil C map corresponds primarily to the carbon content from 0 to 1 meter of soil; we would need first to adjust the observation so that it matches the total soil carbon content that is modeled. Overall, it is a rather complex process to optimize the soil carbon content in the case of ORCHIDEE if we want to keep the internal coherence of the model to improve its predictive skill. Ongoing works are occurring at LSCE to determine the best approach to assimilate soil carbon content observations or potentially turnover time of soil organic matter (derived from observations) into ORCHIDEE.

Similar issues also pertain to the assimilation of forest biomass maps (such as Saatchi et al. 2011). We cannot change easily the above ground biomass in ORCHIDEE without violating the overall carbon allocation scheme and the internal consistency of the model (i.e., the ratio of carbon content between the different reservoirs). We thus would need to perform an optimization of the parameters controlling carbon allocation as well as the input of carbon over a period corresponding at least to the age of the forest. This is a difficult task that was investigated in Thum et al. (in revision) for site scale observations.

The study of Bloom et al. (2016) is slightly different in the sense that the model is less complex than ORCHIDEE and that they could do an optimization over long time period, as needed for carbon stock observations. However, we acknowledge that using carbon stock observations is the next challenge as already mentioned it in the discussion section. For the soil carbon content we thus choose a compromise which is to bring the model to equilibrium in 1990, perform a transient simulation over 10 years and then optimize an ensemble of coefficients that scale (either at site level or globally for several regions) the initial soil carbon content (the slow and passive pools) in order to account for the all past effect that led to deviation from the “equilibrium assumption”.

Second response:

We have improved the text to mention the issues and difficulties to use soil carbon and forest biomass maps with the ORCHIDEE model in order to avoid the classical spin-up approach. In section 2.3.1 we added the following text (that also refers to the discussion in section 4):

“Note that the use of soil carbon data, such as from the Harmonized World Soil Database (as well as above ground biomass data), to initialize the model is not straightforward and represents a challenge to keep the internal model consistency, given that the three soil carbon reservoirs of the CENTURY model are in balance with all components of the model, in particular the input through the different litter pools. Computational and scientific issues to avoid a spin-up approach are still under investigation with ORCHIDEE (see discussion section).”

p. 18 l.6: How is fire simulated during spin-up?

First response:

During spin-up the ORCHIDEE model is run with fires provided by a “generic” fire emission module that is thus not based on the satellite observation of fire occurrence and fire extension. Such simplification is necessary, as we do not have the past history of fire occurrence to guide the spin-up procedure. We have clarified in the text that the inclusion of GFEDv3 fire emission is not used for the model spin-up.

Second response:

No addition

p.26 l.29: perhaps "ecosystem data streams" is more correct (LE is not carbon sensu stricto)

First response:

Indeed LE is not a carbon cycle data stream but it is related to the carbon cycle through the stomatal conductance at the leaf level. In order to keep the word “carbon” we have changed the expression to “carbon cycle – related data streams”

Second response:

No addition

p. 29 l.17: see also Bloom et al. (2016)

First response:

We added the reference “Bloom et al. (2016)”

Second response:

No addition

Response to reviewer 3

General comments :

The manuscript reports development and application of a data assimilation system which is used to produce a version of ORCHIDEE model optimized to reproduce NDVI, net ecosystem exchange and latent heat flux at land validation/flux tower sites and CO₂ seasonality at

background CO₂ monitoring sites. The stepwise optimization approach is proposed as a simplified alternative to optimizing model to fit NDVI, flux tower data and atmospheric CO₂ data simultaneously. Despite splitting the process in several stages authors succeeded to find a set of parameters allowing the model to fit all types of constraints.

The manuscript is well written, and presents an original and valuable contribution. It can be published after minor revision, hopefully addressing the comments listed below.

First response:

We thank the reviewer for his positive review and we describe below how we have address his comments.

General comment 1. In the optimization framework adopted by authors, model parameters optimized at the set of flux tower sites are later extrapolated to whole land surface using available spatial data on vegetation type, weather and soil type information as drivers. The flux tower site optimization is made by combining several sites within same vegetation type in one group, and average flux seasonality is shown to be improved by the optimization. The variability of the fluxes due to soil quality and slope/drainage within same vegetation type is not directly captured by this approach, while some studies (Ise an Sato, 2008) suggest there is a way to address site level differences in productivity potential (edaphic variability) based on remote sensing data. It would be relevant to mention this factor in discussing reasons for remaining spread in the degree of success that can be achieved using one set of model parameters for optimizing fluxes at several sites of same vegetation type.

First response:

We agree that the optimization approach is not able to account for all sources of variability for the carbon and water fluxes measured at FluxNet sites and in particular those linked to edaphic conditions (soil quality, slope and drainage,...). This is indeed a potentially important limitation of current global LSM. The study of Ise and Sato (2008) brings an interesting perspective to include part of the edaphic variability although it relies on strong hypothesis: i.e., the impact of edaphic variability directly controls the vegetation distribution at high spatial resolution and the GLC2000 land cover product is able to capture the differences between high, medium and low productivity ecosystems. The authors have shown that taking into account the spatial variability of the land cover from GLC2000 could significantly improve the model simulation of Leaf Area Index at high latitude in North America, but not really over Siberia.

We thus believe that it is an interesting direction of research, worth to be mentioned in the discussion, but not specific to data assimilation as it concerns the global LSM performance in general. We thus only added in section 4 the following sentence:

“Finally, one can mention new approaches based on remote sensing data to account for site level differences in productivity potential due to edaphic variability (soil quality and slope/drainage) within the same vegetation type (Ise an Sato, 2008).”

Second response:

We slightly revised the sentence added initially to mention that Ise and Sato (2008) only illustrated the potential for high latitude in North America:

“Finally, one can mention new approaches based on remote sensing data to account for site level differences in productivity potential due to edaphic variability (soil quality and

slope/drainage) within the same vegetation type, as illustrated for high latitudes in North America (Ise and Sato, 2008).”

Detailed comments

Page 01 – Line 03. In addition to “incorrect model parameter values” one should mention uncertainty in spatial distribution of the parameters coming from the maps of soil properties, topographic features, vegetation types.

First response:

We agree and have added: “poor description of land surface heterogeneity (soil and vegetation properties),...”

Second response:

No addition

Page 04 – Line 05. Randerson et al (1996) paper can be mentioned among influential studies that use air concentration as constraint

First response:

We agree that Randerson et al. (1996) was a key paper that used atmospheric CO₂ concentration as a constraint to evaluate the impact of specific processes linked to organic matter decomposition. However, this study only used the data to evaluate the model output but not to constraint some parameters with a formal optimization procedure. Given that the introduction is focusing on studies that have used an optimization procedure, we prefer not include Randerson et al. (1996); else we would need to include several other studies that have similarly used atmospheric observations to validate specific ecosystem processes.

Second response:

No addition

Page 04 – Line 26 To extend a list studies using multiple input streams and C stock data in assimilation (Saito et al 2014) can be added.

First response:

We agree that this study was missing from the list of data assimilation studies and we thus added it.

Second response:

No addition

Page 20 Line 13. In many transport models it appears difficult to match CO₂ seasonal cycles in PBL and free troposphere at the same time, which can be attributed to simulated PBL height biases and biases in other processes. The problem can lead to finding a set of model parameters that are optimized well for LMDz model with its PBL height and PBL ventilation rate, but not performing that well when model is different. It would be useful to add figure showing match with free tropospheric data for model validation. Aircraft data and TCCON data can be used for validation, especially high latitude sites know for high seasonal amplitude such as Poker Flats Alaska, or TCCON at Sodankula (Lindqvist et al., 2015). A useful check would include use of vertically integrated profile data at airborne observation

sites (Nakatsuka and Maksyutov, 2009), as it is more stable against the PBL height biases.

First response:

We agree with the reviewer that the representation of the PBL spatial and temporal dynamic is crucial when using atmospheric CO₂ data to optimize ecosystem model parameters or surface fluxes. However, using few scarce free tropospheric data to evaluate the performance of the optimization will not bring significant information as the dynamic of the PBL varies substantially between regions; we thus would need to have a large set of free tropospheric data to provide a comprehensive validation.

The second suggestion of the reviewer concerns vertically integrated data, such as TCCON. Indeed they depend less on PBL height biases, but they however depend crucially on other large-scale uncertain model features, such as the north – south overall mixing.

Finally a technical constraint complicated the evaluation of the model output with these new observations. We indeed used pre-calculated transport fields (model Jacobian) that were calculated at a selected set of surface stations (computationally intensive process) with an older version of LMDz: version 3. It would thus require us to run again the LMDz transport model version 3, which was not feasible in a reasonable time frame period.

Given this technical constraint and the relatively small-expected gain from the evaluation at free tropospheric sites or at TCCON sites, we propose instead to use additional surface stations not used during the optimization (but where the Jacobian are available). We have used 17 sites that are more representative of continental fluxes than the stations that were assimilated and 7 sites that correspond to Pacific Ocean cruises that were left aside in order not to overweight that particular region in the optimization. This independent atmospheric CO₂ evaluation illustrates that the improvement is not only valid at the optimization sites. On average the mean RMSE for the 27 additional sites is 10.5 ppm for the prior of step 1 (prior of ORCHIDEE), 2.8 ppm for the prior or step 3 and 2.1 ppm for the posterior of step 3. The corresponding values for the 53 sites used for the optimization are: 10.5, 2.45, 1.8 ppm, respectively. The error reduction during step 3 is thus similar for both the assimilated and the validation data sets. We added this additional evaluation in the paper (section 3.1.3) as an independent validation of the optimization with selected atmospheric CO₂ observations.

Second response:

We modified the text in order to mention why we have not used aircraft data and TCCON data for validation, even if these free tropospheric data are less dependent on the PBL height. Also when mentioning the use of additional surface stations for validation we now justify why we have not used these particular sites in the optimization.

The text at the end of section 2.2.3 now becomes:

“We also used additional sites to evaluate the result of the optimization (locations indicated in Fig. 3): this included 17 continental sites that are more directly influenced by local fluxes potentially not well captured at the considered LMDz spatial resolution and 7 sites from Pacific Ocean cruises that were not included in the optimization in order not to overweight the data contribution from that particular region. Note that we did not consider free troposphere aircraft data or column integrated measurements (TCCON sites) in this evaluation, although they are less sensitive to biases in the Planetary Boundary Layer representation, given that i) we are using pre-calculated transport fields previously computed at surface stations only, and ii) few scarce free tropospheric datasets will not bring much more information to the additional surface stations.”

Response to reviewer 4

General comments:

The manuscript presents a sequence of parameter estimation exercises for the ORCHIDEE Land Surface Model using a CCDAS data assimilation framework. Firstly, NDVI data are assimilated at point scale. Secondly, FLUXNET data are assimilated at point scale. Thirdly, atmospheric CO₂ data are assimilated at global scale. The presentation of the material is excellent, despite some minor inconsistencies.

First response:

We thank the reviewer for having commented our manuscript. We explain below why we disagree to some of his major comments.

The novelty of the material is limited. What the authors present as a step-wise system, are in fact three systems that are operated in a sequence. The interface between these systems is minimal: It consist of selected parameters with error bars but excluding the error covariance that are passed in one direction. The step-wise approach is not new. It is described, for example, by Rayner et al. (2005): They assimilate NDVI in the first step and atmospheric CO₂ in the second step. The system for assimilation of NDVI is described in more detail elsewhere (MacBean et al., 2015). The system for assimilation of FLUXNET data is described in more detail elsewhere (Kuppel et al., 2012, 2014). What is left is the system for assimilation of a single data stream, i.e. the atmospheric CO₂ data from 2002 to 2004. The description of the assimilation method is provided elsewhere (see above references). The ORCHIDEE LSM, the LMDz CTM and the use of influence functions was also described elsewhere (see references in section 2.3.2). The assimilation of atmospheric CO₂ using a combination of an LSM and a CTM and prescribed emissions from other components of the carbon cycle is not new either. It was presented by Rayner et al. (2005) and applied for a time span of two decades. In summary the manuscript is not suitable for GMD because it fails to present "substantial new concepts, ideas, or methods".

First response:

We disagree with the main criticism that our study does not provide new ideas or methods. In order to explain this further we need to lay out the evolving state of carbon cycle data assimilation.

Systems that apply the well-established methods of data assimilation to models of the carbon cycle at various scales have been around for nearly two decades. Wang et al. (2001) and Kaminsky et al (2002) antecede Rayner et al. (2005). The problem pointed out by Rayner et al. (2010) is that information was not transferable between either different sites or different datastreams. Rayner et al. (2005) for example, did not expose any of the phenological parameters of the assimilation from Knorr et al. (2001) in their assimilation so there could be no test of consistency. Rayner et al. (2010) pointed out that evolution of both models and methods was necessary for comprehensive assimilation. The current paper represents an important step in that evolution though by no means the final one.

- The paper describes for the first time (to our knowledge) a system that is able to assimilate three major carbon cycle data streams (vegetation activity from satellite, FluxNet data and atmospheric CO₂) in a process-based land surface model used as the land component of an Earth System Model (ESM). No such system has been described so far, although this is a major challenge given the differences obtained for the carbon cycle in the last collection of model used for CMIP5 exercise (last IPCC report).
- The reviewer slightly overstates the achievement of Rayner et al. (2005). Although it did use soil moisture and radiation fields from an earlier assimilation from a related model (a simpler version) this was irrelevant to the narrative of that paper. The fields could just as easily have come from a direct satellite product. There was little comment made on the consistency between the two assimilations and no parameters passed between them. Since then, numerous global scale carbon cycle data assimilation studies have been published (above 10) all of them contributing additional aspects to these systems. However in those 10 years a third and crucial data stream, namely the widely used FLUXNET network of net CO₂ and latent heat flux observations, has not yet been included with FAPAR and CO₂ data in a global scale assimilation. All other studies to our knowledge use FAPAR data and CO₂ or FLUXNET data, but none have used all three.
- The focus of the paper lies in the combination of these three data streams while the individual papers MacBean et al. 20015 and Kuppel et al. 2012, 2014 focus on the impact of each individual data stream. The major result of the paper is that for the first time “a state of the art global land surface model part of an ESM is able to capture with a reasonable accuracy the information content of three major data streams following a data assimilation procedure”. This is no insignificant feat as it opens new perspectives to reduce the spread of the land carbon sink simulated by the CMIP5 suite of models and thus to reduce possibly the uncertainty in long-term climate predictions.
- We acknowledge that the chosen approach may not be the optimal one in a statistical sense with only the propagation of the error variance of the optimized parameters (see more detail in the response to the next comment).
- We and the reviewer agree that this is, fortunately, a burgeoning field of activity. Raoult et al (2016) and Schurman et al. (2016) are contemporarily studies, that rely on land surface models of an ESM. They present different strengths and weaknesses from this paper. However we are confident that the paper does represent an advance in available methods. Raoult, et al. (2016) only uses FluxNet observations to optimize the parameters of the JULES model, while Schürmann et al. (in revision) only assimilate two data streams (fAPAR and CO₂) in JSBACH model (at coarse resolution, 10° x 10°). Note finally that the level of complexity of the ecosystem model is part of the problem: achieving an optimization with a simpler model does not guaranty that the framework would work with a more complex one.

Overall, the paper relies on old data assimilation concepts (published way before Rayner et al. 2005) but provides a new implementation (3 data streams with a state of the art component of an ESM) and opens the road for improved carbon – climate coupled simulations and improved climate predictions.

We acknowledge that we have not done enough to highlight the new features of this study, and thus we have emphasized these points in the “introduction” and “discussion and conclusion” sections.

Second response:

We agree that we have not included enough of the text in the above argumentation in the manuscript to justify the novel aspects of our study; we have thus further changed the introduction to emphasize the context so that the reader can see more clearly why this paper represents an important step in the evolution of carbon cycle data assimilation systems. Several changes occurred in different places in the introduction in order to keep the initial logic:

- We first included the study by Kaminski et al. (2002) after the reference to Knorr et al. (1995), adding the sentence:
“Later, Kaminski et al (2002) constrain the seasonal cycle of SDBM with the same data stream.”
- Then after the introduction of Rayner et al. (2005), we completed the description of this important first CCDAS study with the following sentence:
“Note that although Rayner et al. (2005) did use, in addition to atmospheric CO₂ data, soil moisture and radiation fields from an earlier assimilation from a simpler model version, no parameters were passed between the two assimilations and very little comment was made on the consistency between the two assimilations, an important issue that will be central to this paper.”
- Finally, after the introduction of the main objective of our study, we added few sentences to reinforce the novel aspects:
“This study is the first (to our knowledge) to assimilate these three major data streams in a process-based LSM used as the land component of an Earth System Model (ESM), the French Institut Pierre Simon Laplace ESM. Two contemporary studies also optimize the parameters of the land component of an ESM; however Raoult, et al. (2016) only uses FluxNet observations to optimize the parameters of the JULES model, while Schürmann et al. (2016) only assimilate two data streams (fAPAR and CO₂) in the JSBACH model at coarse resolution (10° x 10°). Note finally that the level of complexity of the ecosystem model (and the spatial resolution) is part of the problem: achieving an optimization with a given model does not guarantee that the framework would work with a more complex or different one.”

The scientific approach of passing reduced information on the parameters from one assimilation system to the next is questionable. The reviewer agrees with the author's statement: "It is important to note that this is an implementation question. Tarantola (2005) recasts the fundamentals of the approach as the conjunction or multiplication of probability densities. This multiplication is associative so it makes no difference whether it is performed in one step or several." However, an implementation of such a

step-wise procedure needs to propagate the full Probably Density Function from one step to the next. In the Gaussian framework selected here this requires to propagate the full error covariance matrix and not just the error bars (see comment above). Error correlations are to be expected (see, e.g. Raoult et al., 2016). The change of the parameter space from one step to the next adds a further weakness as well as the dependence of \mathbf{H}_1 on the last iteration of each step. The degradation of the results in the back-compatibility test is no surprise. Another test that has not been performed here would be to operate the sequence of assimilation systems in the reverse order and compare the final parameters and validation results. The computing effort is the same as for the order presented here.

First response:

We agree with the reviewer that with the Gaussian framework it would have been optimal to propagate the full error covariance matrix. We however did not propagate the off-diagonal terms for the following reasons:

- It was a substantial simplification in term of system engineering to only propagate the diagonal terms when we initially built the system.
- The error covariance terms were not large as we obtained correlations that were on average below 0.3.
- Propagating the variances appears to be “sufficient”. This is indirectly verified given that the back-compatibility is achieved to a very good level on average (figure 8). The degradation of the fit is indeed marginal: i) for FluxNet data the change of RMSE between step 2 and step 3 is negligible compare to the improvement achieved during step 2; ii) for NDVI, the change is only significant for Temperate deciduous tree and C3 grasses but the RMSE in step 3 is still much lower than with the prior parameter set. These back-compatibility tests thus indicate that the information provided in previous steps is not lost during subsequent steps.
- Overall, we started this study with only the propagation of the variances from one step to the next, but we also investigated the impact of not propagating the covariance with simpler models and set up. MacBean et al. (2016, in review) analyzed these issues: their main finding is that not propagating the covariance terms is likely to have a small influence on the posterior parameter values. Note finally that since submitting this paper we are working on improving the system to propagate the diagonal terms.

Our approach provides thus a simple step-wise framework that is able to account for the three sources of information with no significant lost of information from one step to the next as revealed in figure 8 and with coherent parameter changes.

However, we acknowledge that this issue was probably not highlighted enough in the original text. We have thus slightly reinforced it in the discussion section and we also mention it in the method section.

Second response:

We have slightly changed the method to justify our choice. The sentence is now: “Note that for simplicity we did not propagate the error correlations in this first implementation of the system, a simplification that appeared sufficient (see the consistency analysis in section 3.2); section 4 also discusses the potential impact of this simplification.”

For the discussion section, we believe that it provides enough detail to the reader with a synthesis of the different points detailed in our first response to the reviewer (see above).

The assimilation of a statistical index, i.e. NDVI, is somewhat beyond state of the art, as assimilation of the related physical variable, FAPAR, has been demonstrated for multiple LSMs (Knorr et al., 2010, Schürmann et al., 2016). The required physical model of FAPAR is available in ORCHIDEE (Naudts et al., 2015).

We strongly disagree with this statement for the following reasons, which have been outlined in Bacour et al. (2015) and MacBean et al. (2015) but we chose not to repeat in this paper so as not to have overlap between the two studies:

- Studies have shown that considerable discrepancies exist between so-called “high-level” satellite products such as LAI or fAPAR, especially when considering their magnitude (D’Odorico et al., 2014; Garrigues et al., 2008; Pickett-Heaps et al., 2014). These differences / uncertainties are attributed to differences in the processing chains, in particular the radiative transfer models that are used to derive these products (based on different physics and assumptions) Figure 1 below, taken from D’Odorico et al. (2014), illustrates the issues with 3 state of the art FAPAR products. The maps highlight the differences in space over Europe, while the frequency distributions for July (at the peak of the growing season) are clearly significantly different between these products.
- We have therefore considered a vegetation greenness index, the Normalized Difference Vegetation Index (NDVI) and we only used the temporal information brought by this product using normalized values. The impact of using raw fAPAR data on the optimized model parameters for ORCHIDEE has been detailed in Bacour et al. (2015). This study shows that the maximum fAPAR values during the peak of the growing season imposes strong constraint on the maximum photosynthetic capacity parameters (VCMAX, VJMAX) which could lead to the estimation of spurious parameter values. Similar results have been obtained by Zobitz et al. (2014) who showed that the assimilation of FAPAR data (alone) could result in unrealistic simulated NEE values.
- Given that fAPAR and NDVI are nearly linearly related and that we normalize the signal between 0 and 1, using one or the other variables is thus equivalent.
- Note finally that Schürmann et al., (2016) obtain a very large impact on the gross and net carbon fluxes with the assimilation of raw fAPAR data; they could not evaluate if it degrades or improves the maximum photosynthetic uptake (at least it pulled the GPP towards values much lower than the data-driven product of Jung et al. (2011) based on FluxNet data).

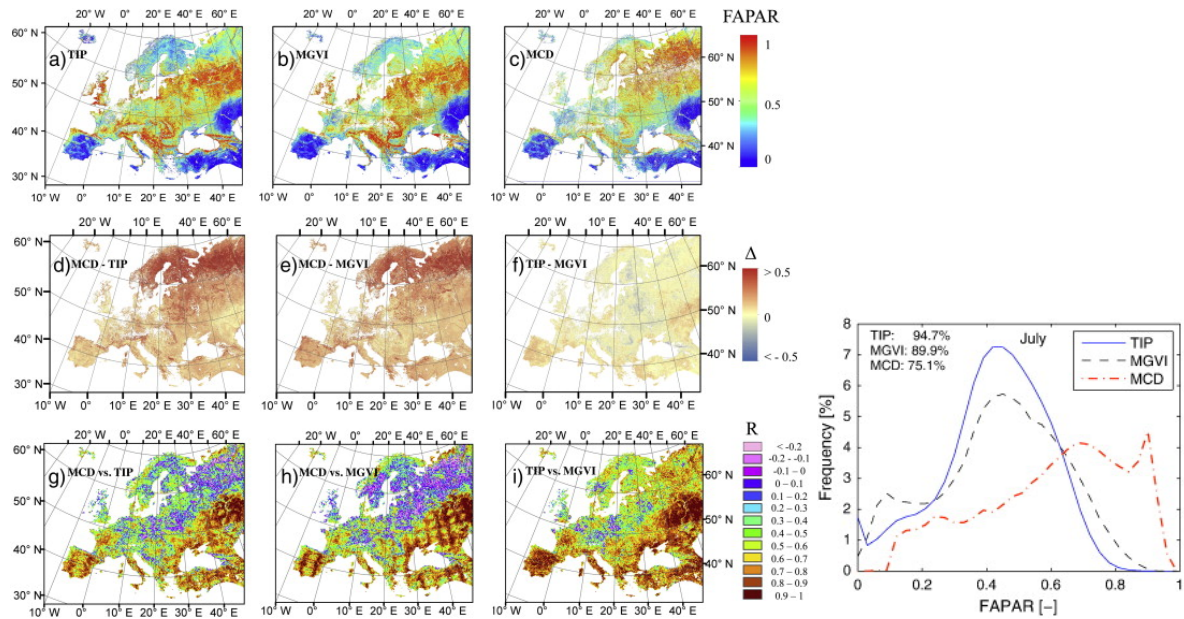


Figure 1 (from D'Odorico et al., 2014): Left: Maps of FAPAR from TIP, MGVI and MCD products (a-c), their differences (d-f), and their correlations (g-i). Temporal resolution: a-f) July monthly composite for the year 2011; g-i) July monthly composite for years 2009–2011. Spatial resolution (pixel size): a-c) 1 × 1 km; d-f) 3 × 3 km; g-i) 18 × 18 km.; Right: FAPAR frequency distributions for TIP, MGVI and MCD products over Europe for July of year 2011.

Overall, we appreciate that we have not discussed enough our choice, given our wish to limit the overlap with MacBean et al. (2015) as mentioned above. So we have now added one sentence in section 2.4.1 to justify more clearly our choice:

“Given that considerable discrepancies exist between so-called “high-level” satellite products such as LAI or fAPAR regarding their magnitude (D'Odorico et al., 2014), we thus only use the temporal information in the NDVI observations and normalized both the model FAPAR output and the NDVI observations to their 5th and 95th percentiles (following Bacour et al. (2015)).”

Note finally that Naudts et al. (2015) describe a version of ORCHIDEE, named ORCHIDEE-CAN, that was not available at the beginning of the study and that has only been validated for European ecosystems (i.e. not the tropical ones for instance).

Second response:

Given the risk of repeating the arguments outlined in Bacour et al. (2015) and MacBean et al. (2015) we have only slightly reinforce the justification mentioned in section 2.4.1. We added one sentence so that the overall justification becomes:

“Given that considerable discrepancies exist between so-called “high-level” satellite products such as LAI or fAPAR when considering their magnitude (D'Odorico et al., 2014), we thus only use the temporal information in the NDVI observations and normalized both the model FAPAR output and the NDVI observations to their 5th and 95th percentiles (following Bacour et al., 2015 and MacBean et al., 2015). Note that assimilating raw fAPAR data with the ORCHIDEE model led to a degradation of the NEE with the estimation of spurious parameter values (Bacour et al., 2015).”

Specific Comments:

p11: 184 parameters is misleading, as none of the three systems estimates that many parameters Why are KsoilC parameters differentiated per region?

First response:

We agree that 184 is the total number of parameters optimized, but that in step 2 and step 3 the number is slightly lower and that in step 1 it is indeed much lower. We have corrected the text to be more precise.

As for the KsoilC parameters, they scale the initial values (after spin-up) of the modeled slow and passive soil carbon pool sizes, in order to take account of all the historical effects not accounted for in the model that would result in a disequilibrium of these pools in reality. It would thus be a strong hypothesis to assume that the “historical effects” impacted the soil carbon content uniformly. Indeed the history of land cover changes and land management largely differ between region/ecosystems and not accounting properly for their impact on soil carbon stock is a crucial point to address. For the global scale optimization step, we used 30 $K_{soilC,reg}$ parameters corresponding to 30 regions (see Fig. A2). Rayner et al. (2005) used a similar approach with 13 coefficients for their 13 PFTs. In our case we choose to define the region not on a PFT basis but following large ecosystems regions that could be coherent for the history of land cover change, land management as well as ecosystem and edaphic conditions. Note that Schurmann et al. (2016) use only one global scalar and recognize that this is one of the major limitations of their approach.

However, we acknowledge that the choice of 30 regions was not enough justified and we thus added one sentence in section 2.3.3: *“For the global scale optimization step, we used 30 $K_{soilC,reg}$ parameters corresponding to 30 regions potentially coherent for land use and land management history as well as ecosystem and edaphic properties (see Fig. A2).”*

Second response:

We did not further change the text of section 2.3.3 from the first response as scaling the initial soil carbon pools is a standard approach used in all carbon cycle data assimilation systems so far.

p23: Why are the FLUXNET assimilations performed per site and not simultaneously? How is the error of the parameter averaged over PFTs calculated.

First response:

We guess the reviewer is asking why the assimilations are performed per PFT and not simultaneously for all PFTs, because all sites were included simultaneously for each PFT in a so-called “multi-site optimization”. The reason for a per PFT optimization was technical as doing it per PFT was slightly simpler and it allowed us to make several tests independently for each PFT. This allowed running smaller “optimization runs” in terms of requested memory and computing time, which proved to be more efficient given some random system failure (due regularly to failure in disk access).

As a drawback, we indeed had to average the estimated values for few global parameters (not dependent of the PFT). For the uncertainty associated to these parameters we

averaged the variances. We have thus improved the text to describe more precisely the treatment of the error for these parameters.

Second response:

We believe that the details provided in section 2.4.1- step 2 clearly answer the question raised by the reviewer.

Eq.(1) in the manuscript does not correspond with Eq. (1) in Tarantola (1987).

First response:

We agree that this was a mistake and drop the reference to Eq. (1) in Tarantola (1987) and replaced by Chapter 4 (where least square problems are described).

Second response:

No addition

p21: After assimilation of atmospheric CO₂ it is no surprise that the trend is close to observations.

First response:

We agree that this is probably the strongest constraint in the optimization and that it is clearly expected that we match the atmospheric CO₂ trend with the optimization of a large set of parameters. We nevertheless kept the sentence but added at the end the term: “as expected”.

Second response:

No addition

p24: Fluxes are calculated from 2000 to 2009. Why are concentrations in Figure 6 not shown over the same time span?

First response:

We have shown in figure 6 only the time period when the atmospheric concentrations are used in the optimization. For the fluxes, given that we wanted to compare with other approaches, such as the Global Carbon Project estimates, we have run the optimized ORCHIDEE model over a longer period to provide a mean estimate over the 2000 decade. Note finally that restricting the period in figure 6 to three years also helps us to see more clearly the improvements in term of seasonal cycle.

Second response:

We added in section 3.1.3 that figure 6 only covers the assimilation period.

For the discussion of the fluxes over the period 2000-2009 we change the introduction to figure 10 in order to justify our choice:

“We ran the optimized model over the full 2000s decade in order to compare with another estimate of the land surface C residual sink from the Global Carbon Project (GCP, Le Quéré et al, 2015) over the same decade.”

p41: 36 regions while in text it is 30.

First response:

It was a mistake.
Corrected

Second response:
No addition

**A new step-wise Carbon Cycle Data Assimilation System
using multiple data streams to constrain the simulated land
surface carbon cycle**

**P. Peylin¹, C. Bacour², N. MacBean¹, S. Leonard¹, P. J. Rayner^{1,3}, S. Kuppel^{1,4}, E.
N. Koffi¹, A. Kane¹, F. Maignan¹, F. Chevallier¹, P. Ciais¹, P. Prunet²**

[1]{Laboratoire des Sciences du Climat et de l'Environnement, UMR 8212 CEA-CNRS-
UVSQ, 91191 Gif-sur-Yvette cedex, France}

[2]{Noveltis, Parc Technologique du Canal, 2 avenue de l'Europe, 31520 Ramonville-Saint-
Agne, France}

[3]{University of Melbourne, 3010, Vic, Melbourne, Australia}

[4]{Grupo de Estudios Ambientales, IMASL-CONICET/Universidad Nacional de San Luis,
San Luis, Argentina}

Correspondence to: P. Peylin (philippe.peylin@lsce.ipsl.fr)

Abstract

Large uncertainties in Land surface models (LSMs) simulations still arise from inaccurate forcing, poor description of land surface heterogeneity (soil and vegetation properties), incorrect model parameter values and incomplete representation of biogeochemical processes. The recent increase in the number and type of carbon cycle related observations, including both in situ and remote sensing measurements, has opened a new road to optimize model parameters via robust statistical model-data integration techniques, in order to reduce the uncertainties of simulated carbon fluxes and stocks. In this study we present a Carbon Cycle Data Assimilation System (CCDAS) that assimilates three major data streams, namely MODIS-NDVI observations of vegetation activity, net ecosystem exchange (NEE) and latent heat (LE) flux measurements at more than 70 sites (FLUXNET), and atmospheric CO₂ concentrations at 53 surface stations, in order to optimize the main parameters of the ORCHIDEE LSM (around 180 parameters in total). The system relies on a step-wise approach that assimilates each data stream in turn, propagating the information gained on the parameters from one step to the next.

Overall, the ORCHIDEE model is able to achieve a consistent fit to all three data streams, which suggests that current LSMs have reached the level of development to assimilate these observations. The assimilation of MODIS-NDVI (step 1) reduced the growing season length in ORCHIDEE for temperate and boreal ecosystems, thus decreasing the global mean annual gross primary production (GPP). Using FLUXNET data (step 2) led to large improvements in the seasonal cycle of the NEE and LE fluxes for all ecosystems (i.e., increased amplitude for temperate ecosystems). The assimilation of atmospheric CO₂, using the atmospheric transport model LMDz (step 3), provides an overall constraint (i.e., constraint on large scale net CO₂ fluxes), resulting in an improvement of the fit to the observed atmospheric CO₂ growth rate. Thus the optimized model predicts a land C sink of around 2.2 PgC.yr⁻¹ (for the 2000-2009 period), which is more compatible with current estimates from the Global Carbon Project (GCP) than the prior value. The consistency of the step-wise approach is evaluated with back-compatibility checks. The final optimized model (after step 3) does not significantly degrade the fit to MODIS-NDVI and FLUXNET data that were assimilated in the first two steps, suggesting that a stepwise approach can be used instead of the more “challenging” implementation of a simultaneous optimization in which all data streams are assimilated together. Most parameters, including the scalar of the initial soil carbon pool size, changed

during the optimization with a large error reduction. This work opens new perspectives for better predictions of the land carbon budgets.

1 Introduction

Atmospheric CO₂ concentrations have increased at an unprecedented rate over the last few decades, predominantly due to anthropogenic fossil fuel and cement emissions, as well as land use and land cover change (LULCC). The oceans and the terrestrial biosphere have absorbed CO₂, removing on average 50% of anthropogenic emissions from the atmosphere. However, knowledge about the exact location of sources and sinks of carbon (C) and the driving mechanisms is still lacking. Land surface models (LSMs) can be used to improve our understanding of the spatio-temporal patterns of sources and sinks, as well as for attributing changes due to CO₂, climate variability and other environmental drivers. However, the spread in the model predictions of terrestrial net C exchange currently has the same order of magnitude as the uncertainty of the terrestrial C budget estimated as the residual of the other carbon cycle components (Le Quéré et al., 2015). In addition to uncertainties in the mean global annual terrestrial C budget and its trend over time (Sitch et al., 2015), there remain strong discrepancies between LSMs in their predictions of regional budgets (Canadell, 2013) at seasonal and inter-annual timescales and in their sensitivity to climate and atmospheric CO₂ forcing (Piao et al., 2013).

Uncertainties in model simulations arise from inaccurate forcing, incorrect model parameter values and/or an inadequate or incomplete representation of biogeochemical processes in the model (for example the impact of nutrient limitation on C fluxes, or C release related to permafrost thawing). Arguably the best way to improve model predictions is to confront simulations with multiple sources of data within an appropriate and rigorous framework (Prentice et al., 2015). In the last two decades significant efforts by the site and satellite observation communities have resulted in a large increase in the number and type of C cycle-related observations. These data contain some information at various spatial and temporal scales and should be combined together to robustly address different aspects of the models. One way in which these data can be used to better quantify and reduce model uncertainty is by optimizing or calibrating the model parameters via robust statistical model-data fusion (or data assimilation – DA) techniques. In particular a Bayesian inference framework allows us to

update our prior knowledge of the parameters based on new information contained in the observations.

There is a long history of using DA techniques for parameter optimization, particularly in Geophysics (Tarantola, 1987), but the initial studies in the field of global terrestrial C cycle data assimilation started with the initial study of Fung et al. (1987) and a pioneering work by Knorr and Heimann (1995) who used atmospheric CO₂ concentration to constrain the Simple Diagnostic Biosphere Model (SDBM). Later, Kaminski et al (2002) constrain the seasonal cycle of SDBM with the same data stream. This effort was continued by the original Carbon Cycle Data Assimilation System (CCDAS) described in Rayner et al. (2005) and Kaminski et al. (2012) which used both atmospheric CO₂ and satellite-derived Fraction of Absorbed Photosynthetic Radiation (FAPAR) data to optimize vegetation productivity by adjusting the C cycle-related parameters of the Biosphere Energy-Transfer Hydrology (BETHY) model (see a review in Kaminski et al., 2013). Note that although Rayner et al. (2005) did use, in addition to atmospheric CO₂ data, soil moisture and radiation fields from an earlier assimilation from a simpler model version, no parameters were passed between the two assimilations and very little comment was made on the consistency between the two assimilations, an important issue that will be central to this paper. Meanwhile substantial efforts have been put into the use of local eddy covariance flux tower measurements of net exchange of CO₂ and latent and sensible heat fluxes to optimize photosynthesis, respiration and energy-related parameters of terrestrial ecosystem models, both at individual sites (e.g. Wang et al., 2001, 2007; Williams et al., 2005; Braswell et al., 2005; Knorr and Kattge, 2005; Moore et al., 2008; Ricciuto et al., 2008), and more recently using multiple sites together (hereafter multiple sites) from the global FLUXNET network (e.g. Groenendijk et al., 2011; Kuppel et al., 2012, 2014; Alton, 2013; Xiao et al., 2014). Increasingly the focus in carbon cycle data assimilation is moving towards using multiple different data streams as independent constraints, with the aim of bringing more information at different spatial and temporal scales and constraining several processes at once in order to reduce the likelihood of model equifinality (where multiple sets of parameters achieve the same reduction in model-data misfit). Recent examples include the combination of in-situ eddy covariance flux observations and ground-based information on vegetation structure and C stocks (Richardson et al., 2010; Ricciuto et al., 2011; Keenan et al., 2012, 2013; Thum et al., 2015), or in-situ flux data and satellite FAPAR (Kato et al., 2013; Zobitz et al., 2014; Bacour et al., 2015) or atmospheric CO₂ and biomass data using a simple biosphere model (Saito et al., 2014). This is

a non-trivial task however, especially when optimizing a complex LSM (see MacBean et al, submitted), which has many parameters acting from local to global scales.

When assimilating multiple different data streams we have two options: i) to optimize the model with each data stream in turn, and to propagate the information gained on the parameter values from one step to the next (hereafter referred to as “stepwise” assimilation), or ii) to include all data streams together in the same optimization (hereafter referred to as “simultaneous” assimilation). Kaminski et al. (2012) suggested that it is essential to perform a consistent, simultaneous assimilation that includes all data streams in the same optimization. It is important to note that this is an implementation question. Tarantola (2005) recasts the fundamentals of the approach as the conjunction or multiplication of probability densities. This multiplication is associative so it makes no difference whether it is performed in one step or several (and whether the system is linear or not). In complex problems such as these, one cannot carry or even describe the full structure of the relevant probability densities so which approach will work best in each case is unclear. In particular, technical difficulties associated with the different number of observations for each data stream and the characterization of error correlations between them, in addition to computational constraints to run global LSMs, might result in the preference for a step-wise assimilation framework. Additionally, it may be more straightforward, to expose a restricted set of parameters (following a global sensitivity analysis) to each observation type in a stepwise approach to ensure that each data stream constrains only the most relevant parts of the model. This reduces biases from other poorly-represented processes caused by inadequate model structure. Note finally that more complex approaches based on random generation of parameter sets, such as the multi-objective approach using the Pareto ranking of several cost functions (e.g. Yapo et al., 1998), are not yet affordable for global LSMs from a computational point of view. For these reasons we follow the stepwise approach in this paper.

We present the first global-scale CCDAS that assimilates three of the main global data streams that have been used to date to understand the terrestrial carbon cycle – atmospheric CO₂ concentration, satellite-derived information of vegetation greenness (from the MODIS instrument) and multisite eddy covariance net CO₂ and latent heat flux measurements (from FLUXNET) – to optimize the parameters of the Organizing Carbon and Hydrology in Dynamics Ecosystems (ORCHIDEE) process-based LSM (Krinner et al., 2005). This study is the first (to our knowledge) to assimilate these three major data streams in a process-based

1 LSM used as the land component of an Earth System Model (ESM), the French Institut Pierre
2 Simon Laplace ESM. Two contemporary studies also optimize the parameters of the land
3 component of an ESM; however Raoult, et al. (2016) only uses FluxNet observations to
4 optimize the parameters of the JULES model, while Schürmann et al. (2016) only assimilate
5 two data streams (fAPAR and CO₂) in the JSBACH model at coarse resolution (10° x 10°).
6 Note finally that the level of complexity of the ecosystem model (and the spatial resolution) is
7 part of the problem: achieving an optimization with a given model does not guarantee that the
8 framework would work with a more complex or different one.

9 In this context, the main questions that we aim to answer in this paper are as follows:

- 10 i) How and to which extend the optimization of the ORCHIDEE model allows to fit the three
- 11 data streams that are considered?
- 12 ii) Does the step-wise optimization result in a degradation of the fit to other data streams used
- 13 in the previous steps?
- 14 iii) What are the main changes in the optimized parameters when using sequentially these
- 15 three data streams in a global CCDAS and which processes are constrained?
- 16 iv) What are the improvements for the land C cycle in terms of net/gross fluxes and stocks as
- 17 a result of multi-data stream optimization? What preliminary perspectives can we draw that
- 18 may help us in improving model predictions of trends, variability and the location of
- 19 terrestrial C sources and sinks?

20 Following these objectives, the paper first describes the new ORCHIDEE-CCDAS including
21 the concept, the observations, the models and the optimization approach. We then present the
22 results, including the fit to the data, consistency checks (question i) above) as well as mean
23 global and regional C cycle budget for the period 2000-2009. The last section discusses issues
24 and perspectives associated with these results.

26 **2 Methods**

27 **2.1 ORCHIDEE-CCDAS concept**

28 We have designed a CCDAS around the ORCHIDEE land surface model (ORCHIDEE-
29 CCDAS, later also referred to as ORCHIDAS for simplicity) that combines a state-of-the-art

Philippe Peylin 15/8/16 16:30

Supprimé: T

description of the driving biogeochemical processes within the model with multiple observational constraints in a robust statistical framework, in order to improve the simulation of land carbon fluxes and stocks. The system allows us to retrieve the best estimate, given the observations and prior information, of selected parameters (see §2.3.3) as well as to evaluate their uncertainty. It relies on a stepwise assimilation of a comprehensive set of three C cycle-related observations that are representative of small (100 m) to large (continental) scales (see §2.2):

- Step 1: Satellite measurements of vegetation activity using the Normalized Difference Vegetation Index (NDVI) from the MODIS instrument over the 2000-2008 period for a randomly selected set of sites for boreal and temperate deciduous vegetation types;
- Step 2: In-situ eddy-covariance net CO₂ and water (latent heat) flux measurements from the FLUXNET database for a large set of sites, spanning 7 different vegetation types;
- Step 3: In-situ monthly atmospheric surface CO₂ concentration measurements from the GLOBALVIEW-CO₂ database over three years (2002-2004).

The system relies on two models:

- The ORCHIDEE global LSM, whose main C cycle parameters are optimized (see §2.3)
- The atmospheric transport model, LMDz (see §2.3), to relate the surface carbon fluxes to atmospheric CO₂ concentrations.

The framework combines the different observational data streams within ORCHIDAS in order to optimize selected model parameters using a variational data assimilation system, described in section 2.4. Figure 1 illustrates the structure of the CCDAS and the different components that are involved. Such a framework distinguishes i) the assimilated observations, ii) an ensemble of forcing and input data streams, iii) the models and optimization framework, as well as iv) an evaluation step, where independent datasets are compared to the optimized model stocks and fluxes. As explained in the introduction, a major feature of the current system is the stepwise approach, in which all data streams are assimilated sequentially (i.e. one after the other). The information retrieved at a given step (retrieved optimal parameter values and associated uncertainty) is propagated to the next step (see Fig. 2 and §2.4). Note that for simplicity we did not propagate the error correlations in this first implementation of

the system, [a simplification that appeared sufficient](#) ([see the consistency analysis in section 3.2](#)); section 4 [also](#) discusses the potential impact of this simplification.

At each step, the parameter optimization relies on a Bayesian framework that explicitly minimizes the difference between the simulated and observed quantities in addition to minimizing the difference between the optimized model parameters and “a priori” values (see §2.4.2). The dependence of the simulated quantities on the optimized variables is non-linear, which thus necessitates the use of an iterative algorithm. Note that all components of the surface C budget need also to be included in the ORCHIDAS, particularly when using atmospheric CO₂ measurements which requires the atmospheric transport model to be prescribed with fossil fuel emissions, CO₂ fluxes associated with biomass burning and ocean CO₂ fluxes (see §2.5) in addition to net ecosystem exchange (NEE) from ORCHIDEE.

2.2 Assimilated observations

2.2.1 MODIS-NDVI

MODIS collection 5 obtained from surface reflectance data (from 2000-2008) in the red (R) and near-infrared (NIR) bands at 5 km resolution (CMG) are used to optimize the phenology-related parameters of ORCHIDEE in the first step. The R and NIR data were processed to correct for directional effects following Vermote et al. (2009) and then used to calculate the NDVI, which is assumed to be linearly related to the model FAPAR. The NDVI are then i) aggregated to the 0.72° spatial resolution of the ERA-Interim meteorological fields that are used to force ORCHIDEE, ii) interpolated to a daily time series ([for practical implementation](#)) and iii) checked for quality (see MacBean et al., 2015 for details). If there is a gap in the observations of more than 15 days, no interpolation is done (i.e., no data during the gap are assimilated). Figure 3 displays the location of the sites that were selected (see §2.4.1).

2.2.2 Eddy covariance flux data

Eddy covariance flux measurements of net surface CO₂ flux – hereafter referred to as net ecosystem exchange (NEE) and latent heat flux (LE) – from 78 observation sites of a network of regional networks (FLUXNET; see Fig. 3) are used to constrain ecosystem physiology and fast C-related processes at daily to seasonal timescales in ORCHIDEE in the second step. We use quality-checked and gap-filled data from a global synthesis called the La Thuile dataset (Papale, 2006). In order to avoid dealing with the large error correlations in the half-hourly

data (see Lasslop et al., 2008), daily mean values of NEE and LE are used in the ORCHIDAS. Days with less than 80% of the half-hourly data are left out of the assimilation. The selection of the sites and the data processing (gap-filling, correction for energy balance closure) are detailed in Kuppel et al. (2014). Note that uncertainties due to incomplete sampling of the diurnal cycle are likely very small (less than 5%) as the error in the gap-filling procedure is usually less than 20% (Lasslop et al., 2008).

2.2.3 Atmospheric CO₂ concentrations

Atmospheric CO₂ concentration measurements were taken from an ensemble of selected surface stations around the world (Fig. 3). The spatial concentration gradients relate to the integral of the fluxes over large areas and thus allow the optimization of large-scale global patterns of carbon fluxes. These data were taken from the NOAA Earth System Laboratory (ESRL) GLOBALVIEW-CO₂ collaborative product (GLOBALVIEW-CO₂, 2013) and averaged to monthly means. We assimilated the monthly values for 53 sites for the 2002-2004 period inclusive in the last step of the assimilation system. Such restricted period (3 years only) was chosen for practical reasons (computing resources) while constructing the ORCHIDAS system. The station locations, indicated in Fig. 3, favor the background conditions i.e. the surrounding air masses are only weakly influenced by local continental sources, such as power plants. The choice of monthly mean is related to the use of pre-calculated transport fields with LMDZ (see §2.3.2). We also used additional sites to evaluate the result of the optimization (locations indicated in Fig. 3): this included 17 continental sites that are more directly influenced by local fluxes potentially not well captured at the considered LMDZ spatial resolution and 7 sites from Pacific Ocean cruises that were not included in the optimization in order not to overweight that the data contribution from that particular region. Note that we did not considered free troposphere aircraft data or column integrated measurements (TCCON sites) in this evaluation, although they are less sensitive to biases in the Planetary Boundary Layer representation, given that i) we are using pre-calculated transport fields previously computed at surface stations only and ii) few scarce free tropospheric datasets will not bring much more information to the additional surface stations.

Philippe Peylin 13/8/16 22:59

Supprimé: representative of

Philippe Peylin 13/8/16 23:01

Supprimé: continental

Philippe Peylin 19/8/16 22:39

Supprimé: left aside

Philippe Peylin 19/8/16 22:39

Supprimé: particular region in the optimization

2.3 Models and optimized parameters

2.3.1 ORCHIDEE land surface model

In this study we use the ORCHIDEE process-oriented land surface model (Krinner et al., 2005), which computes water, carbon and energy balances at the land surface on a half hourly time step, using a mechanistic description of the physical and biogeochemical processes (see, <http://labex.ipsl.fr/orchidee/>). The model describes the exchange of carbon and water at the leaf level, the allocation of carbon within plant compartments (leaves, roots, heartwood and sapwood), the autotrophic respiration, the production of litter, the plant mortality and the degradation of soil organic matter (CENTURY model; Parton et al., 1988). The hydrological processes for the soil reservoir rely on a double bucket scheme (Ducoudré et al., 1993). The link between the water and carbon modules is via photosynthesis, which is based on the leaf-scale equations of Farquhar et al. (1980) for C3 plants, and Collatz et al. (1992) for C4 plants, that are then integrated over the canopy by assuming an exponential attenuation of light. The FAPAR by each layer of the canopy is calculated from the leaf area index (LAI) following a Beer-Lambert extinction law (Bacour et al., 2015).

ORCHIDEE uses the concept of the plant functional type (PFT) to describe the vegetation distribution, with 13 PFTs (including bare soil) that can co-exist in each grid cell. Except for the phenology (see a recent description in MacBean et al., 2015), the equations governing the different processes are generic, but with specific parameter values for each PFT. Detailed descriptions of model equations can be found in numerous publications (see for instance Krinner et al., 2005). ORCHIDEE can be run at either global scale on a grid, or at site-level using point-scale surface meteorological forcing variables. It is the land surface component of the Institut Pierre Simon Laplace (IPSL) Earth System Model, and the version that we used corresponds to CMIP5 simulations in the IPCC 5th Assessment Report (Dufresne et al., 2013). However, in this study the model is run offline using the ERA-Interim 3-hourly near surface meteorological forcing fields (Dee et al., 2011) aggregated at the spatial resolution of the atmospheric transport model for the global simulations (2.5° x 3.75°; see § 2.3.2). However, when we assimilate in situ flux data in the second step, we force the model with the gap-filled half-hourly meteorological data measured at each site. The global PFT map was derived from the high-resolution IGBP AVHRR land data set (Vérant et al., 2004). The carbon pools are brought to equilibrium (spin-up procedure) for both site and global scale simulations by cycling the available meteorological forcing over several millennia, to ensure that the long-

term net carbon flux is close to zero. For the global simulation in the third step, we spun-up the model recycling the 1989-1998 meteorology and then used a transient simulation from 1990 to 2001 with changing climate (ERA-Interim) and increasing CO₂, before starting the optimization with atmospheric data over 2002-2004. For the site simulations (i.e., the assimilation of flux data) we recycled the available in situ meteorological forcing to spin-up the model, with present day CO₂. Note that the use of soil carbon data, such as from the Harmonized World Soil Database (as well as above ground biomass data), to initialize the model is not straightforward and represents a challenge to keep the internal model consistency, given that the three soil carbon reservoirs of the CENTURY model are in balance with all components of the model, in particular the input through the different litter pools. Computational and scientific issues to avoid a spin-up approach are still under investigation with ORCHIDEE (see discussion section).

2.3.2 LMDz model

The transport model used in this study is version 3 of the General Circulation Model (GCM), LMDz (Hourdin and Armengaud, 1999) with a horizontal resolution of 3.75° (longitude) x 2.5° (latitude) and 19 sigma-pressure layers up to 3 hPa. The calculated winds (u and v) are relaxed to the ECMWF ERA-40 meteorological data (Uppala et al. 2005) with a relaxation time of 2.5h (guiding) in order to realistically account for large-scale advection (Hourdin et al., 2000). Deep convection is parameterized according to the scheme of Tiedtke (1989) and the turbulent mixing in the planetary boundary layer is based on a local second-order closure formalism. The LMDz GCM model has been widely used to model climate (IPCC, 2007, 2013) and its derived transport model has been used for the simulation of chemistry of gas and particles and greenhouse gases distributions (Hauglustaine et al., 2004; Folberth et al., 2005; Bousquet et al. 2005, 2006; Rivier et al., 2006). For this study, we used pre-calculated transport fields, as described in Peylin et al. (2005), that correspond to the sensitivity of concentration at each atmospheric site and each month to the surface flux of each model grid-cell for each day (often called influence functions). The sensitivities (using inter-annual winds) were calculated with the “retro-transport” formulation implemented in the LMDz transport model (Hourdin et al. 2006). This approach decreases the computing time of the optimization compared to the use of the full forward LMDz model at each iteration, as the transport is replaced by a matrix multiplication with the vector of surface fluxes. Note that the initial 3D state of the atmospheric concentrations was defined from Chevallier et al. (2010)

2.3.3 Parameters optimized

The optimized parameters are described in Table 1, and their prior values, uncertainty and range are given in Table 2. In the most recent studies using ORCHIDAS at site scales a large set of ORCHIDEE parameters has been optimized (Kuppel et al., 2014; Santaren et al., 2014; Bacour et al., 2015). In this study a smaller set was chosen, based on a Morris sensitivity analysis (Morris, 1991; results not shown) that determines the sensitivity of the NEE and LE to all model parameters at various FLUXNET sites (for each PFT), in order to reduce the computational cost of the global optimization in step 3 (see §2.5). We considered PFT-dependent and 4 “global” (i.e. non PFT-dependent) parameters that control mostly the fast carbon processes (diurnal to seasonal). In addition, we introduced a new parameter, K_{soilC} , to scale the initial values (after spin-up) of the modeled slow and passive soil carbon pools, in order to take account of all the historical effects not accounted for in the model that would result in a disequilibrium of these pools in reality. For the site-specific optimizations with FLUXNET data, we have one $K_{soilC,site}$ parameter per site. For the global scale optimization step, we used 30 $K_{soilC,reg}$ parameters corresponding to 30 regions potentially coherent for land use and land management history as well as ecosystem and edaphic properties (see Fig. A2). The initial soil carbon pools of all pixels within each region were thus scaled by the same value. The prior value for all K_{soilC} parameters was set to one, i.e. the default state of soil carbon pools is assumed to be in equilibrium.

Overall (including all PFT-dependent parameters), we optimize 16 parameters related to phenology, 36 to photosynthesis, 3 to respiration, 1 to the energy budget, 78 soil C pool scalars (one for each FLUXNET site), and 30 regional soil C pool scalars for the global simulations – a total of 184 parameters (16, 134 and 86 in step 1, 2 and 3, respectively). Note that the soil C pool multipliers at the FLUXNET sites are independent from the regional C pool multipliers, as the history of soil carbon over large eco-regions of several millions square kilometers is rather heterogeneous (as it is mainly related to previous land use changes), and most likely, the FLUXNET sites are not representative of larger regions in terms of the soil carbon disequilibrium. The prior standard deviation for each parameter is equal to 40% of the parameter range (lower and higher boundaries) prescribed for each parameter following Kuppel et al. (2012). The parameter ranges were specified following expert judgment of their meaning in the ORCHIDEE equations and based on literature reviews or databases (such as TRY, Kattge et al., 2011).

2.4 System description: a step-wise approach

2.4.1 Stepwise assimilation of three data streams

The ORCHIDAS system relies on a stepwise assimilation of the three data streams described in section 2.2. Figure 2 illustrates the flow of information in this sequential approach:

Step 1 – Assimilation of MODIS-NDVI: Four parameters related to the seasonal cycle of the vegetation (phenology) are optimized for the temperate and boreal deciduous PFTs (TeBD, BoND, BoBD and NC3 – see caption of Table 2). These four deciduous PFTs alone are considered in step 1 in this ORCHIDAS version because the tropical deciduous phenology modules in ORCHIDEE require further modifications to improve the functions that control leaf growth and fall in response to water availability (MacBean et al., 2015). Evergreen PFTs were also not considered, as there are no phenology modules related to these PFTs in the model. The procedure is similar to that described in detail in MacBean et al. (2015) and therefore only briefly recalled here. A simple linear relationship between the modeled Fraction of Absorbed Photosynthetically Active Radiation (FAPAR) and MODIS-NDVI observations is assumed, based on studies such as Knyazikhin et al. (1998). Given that considerable discrepancies exist between so-called “high-level” satellite products such as LAI or FAPAR when considering their magnitude (D’Odorico et al., 2014), we thus only use the temporal information in the NDVI observations and normalized both the model FAPAR output and the NDVI observations to their 5th and 95th percentiles (following Bacour et al., (2015) and MacBean et al., 2015). Note that assimilating raw fAPAR data with the ORCHIDEE model led to the degradation of the NEE with the estimation of spurious parameter values (Bacour et al., 2015). The model was run for fifteen randomly selected grid cells for each of the four PFTs using the ERA-Interim meteorological forcing. Only grid cells that included vegetation fraction of greater than 60% for the PFT optimized were considered. We selected a set of grid points instead of the whole grid to substantially decrease the computing time; but the remaining points are used for the evaluation of the optimized model. The fifteen sites for each PFT were included in one optimization for each PFT following a multi-site approach, in which all observations are used simultaneously to optimize the model parameters. The optimized parameters are described in Table 1. They correspond to a scalar on the growing degree days (GDD) threshold for the start of the vegetation ($K_{pheno,crit}$), a parameter controlling the use of carbohydrate reserve during the start of leaf growth

($K_{lai, happy}$), a temperature threshold for the onset of leaf senescence (CT_{senes}) and the critical age for leaves ($L_{agecrit}$).

Step 2 – Assimilation of FLUXNET data: Mean daily NEE and LE flux measurements for 78 sites, including up to 10 years worth of data for each site, are used to optimize a set of model parameters controlling the fast carbon and water processes (photosynthesis, respiration, phenology – see Table 1). The site selection and the choice of a daily time step are described in more details in Kuppel et al. (2014). These sites cover 7 of the PFTs in ORCHIDEE (see Table 2). The posterior parameter values of the four phenology parameters derived in step 1, and their associated uncertainties, are input as prior information in step 2. For the additional parameters, the default ORCHIDEE values are used for the prior and the uncertainties are set as described in §2.3.3. A multi-site optimization is performed for each PFT independently as in step 1. Global parameters, i.e. those that are not PFT-dependent, were optimized for each PFT and the mean across all PFTs was then calculated to define the prior parameter vector in step 3 of the assimilation with atmospheric CO₂ data (at global scale). Such an approach was chosen to allow us to optimize all PFTs in parallel and therefore to simplify the assimilation process.

Step 3 – Assimilation of atmospheric CO₂ concentrations: We use monthly mean CO₂ concentrations from 53 surface stations over three years (2002-2004) to provide a large-scale constraint to the land surface fluxes (i.e. to match the global CO₂ growth rate, mean seasonal cycle and its latitudinal variation, as well as the spatial gradients between stations). We use the LMDz atmospheric transport model (see §2.3.2) to assimilate these observations. The set of parameters optimized in step 2 are included in step 3, except for the albedo scaling parameter ($K_{albedo, veg}$), as the net carbon fluxes are only weakly sensitive to that parameter. We used the posterior parameter distributions from step 2 (parameter optimal values and associated uncertainties) as prior information for step 3, and expanded the parameter vector to include the 30 K_{soilC} parameters that scale the initial soil carbon pools for large “spatially-coherent regions” (see §2.1.2 and Fig. A2). The air-sea fluxes and fossil fuel and biomass burning emissions are also accounted for (but not optimized) in this final step, in order to close the global carbon budget within the atmospheric transport model (see §2.5).

2.4.2 Optimization procedure (for all steps):

In each step the statistically optimal parameter values are derived with an optimization procedure following the principle of the 4-D variational assimilation systems (developed for numerical weather prediction), using a tangent linear operator (and finite differences for a few parameters, Bacour et al. 2015). Assuming that the errors associated with the parameters, the observations and the model outputs follow Gaussian distributions, the optimal parameter set corresponds to the minimum of a cost function, $J(\mathbf{x})$, that measures the mismatch between i) the observations (\mathbf{y}) and the corresponding model outputs, $H(\mathbf{x})$, (where H is the model operator), and ii) the a priori (\mathbf{x}_b) and optimized parameters (\mathbf{x}), weighted by their error covariance matrices (Tarantola, 1987; Chapter 4):

$$J(\mathbf{x}) = \frac{1}{2} \left[(H(\mathbf{x}) - \mathbf{y})^T \mathbf{R}^{-1} (H(\mathbf{x}) - \mathbf{y}) + (\mathbf{x} - \mathbf{x}_b)^T \mathbf{B}^{-1} (\mathbf{x} - \mathbf{x}_b) \right] \quad (1)$$

\mathbf{R} represents the error variance/covariance matrix associated with the observations and \mathbf{B} the parameter prior error variance/covariance matrix. At each step a different cost function is defined with the observations and parameters related to that step (see Fig. 2). \mathbf{R} includes the errors on the measurements, the model structure and the meteorological forcing. Model errors are rather difficult to assess and may be much larger than the measurement error itself. Therefore we chose to focus on the structural error and defined the variances in \mathbf{R} as the mean squared difference between the prior model and the observations for both step 1 and step 2 (see Kuppel et al. 2013). For simplicity we assumed that the observation error covariances were independent between the different observations and therefore we kept \mathbf{R} diagonal (off-diagonal terms set to zero), given the rapid decline of the model error auto-correlation beyond one day (Kuppel et al., 2013). For step 3 we used a different approach, given the large bias in the model a priori concentrations, and therefore followed the methodology of Peylin et al. (2005) based on the observed and modeled temporal concentration variability at each site. Overall, data uncertainties in the optimization procedure are between 0.1 and 0.45 for NDVI (step 1), around 3-6 gCm⁻²d⁻¹ for daily NEE, and 15-30 Wm⁻² for daily LE (step 2) and between 0.1 ppm at remote oceanic stations and 4 ppm at continental sites (step 3).

The determination of the optimal parameter vector that minimizes $J(\mathbf{x})$ is performed by successive calls to a “gradient-descent” minimization algorithm L-BFGS-B (Byrd et al. 1995), which is specifically dedicated to solving large nonlinear optimization problems that are subject to simple bounds on the parameter values. In order to find the minimum of $J(\mathbf{x})$ the

algorithm requires the gradient of $J(\mathbf{x})$ (Jacobian) with respect to the ORCHIDEE parameters. L-BFGS-B explores each parameter space simultaneously along the gradient of the cost function, and uses an approximation of the Hessian (second derivative) of $J(\mathbf{x})$, which is updated at each iteration, to define the size of the step at each iteration.

For step 1 and step 2, the model “ H ” simply corresponds to the land surface model: $H = S$, with $S(\mathbf{x})$ representing the surface fluxes from the ORCHIDEE model using the parameter vector, \mathbf{x} . The gradients $dJ(\mathbf{x})/d\mathbf{x}$ are calculated from the tangent linear model of ORCHIDEE that was automatically generated by the numerical Transformation of Algorithms in Fortran (www.fastopt.de), except for two parameters linked to the model phenology for which the threshold functions prevent the use of a linear approximation. A finite difference approach was used for these parameters in order to define a mean derivative at any point; we also checked that no spurious oscillations occurred for these parameters during the minimization iterations.

For step 3, the model “ H ” corresponds to the composition of the land surface model with the transport model: $H = T \circ S$ (see Kaminski et al. (2002) for details), with T representing the LMDz transport model. T is a linear operator for a non-reactive species: $T(S(\mathbf{x})) = \mathbf{T} \cdot S(\mathbf{x})$, with \mathbf{T} a matrix representation of the transport operator. It corresponds to the sensitivity of CO_2 concentrations at each site and for each month to the daily surface flux of each model grid-cell. It is then combined with the ORCHIDEE surface fluxes ($S(\mathbf{x})$) through a matrix multiplication to derive $H(\mathbf{x})$. \mathbf{T} has been pre-calculated for all atmospheric stations in order to save computing time during the iterative optimization process (see §2.3.2). For simplicity we use monthly mean values for both the fluxes $S(\mathbf{x})$ and the transport sensitivities (\mathbf{T}) in the computation of the gradients $dJ(\mathbf{x})/d\mathbf{x}$.

For improved minimization efficiency, the inversion is preconditioned (following Chevallier et al., 2005), which means that L-BFGS-B is fed with the control variable $\mathbf{x}' = \mathbf{B}^{-1/2}(\mathbf{x} - \mathbf{x}_b)$, rather than with \mathbf{x} , as this homogenizes the range of variation of the optimized parameters.

2.4.3 Error estimation

The posterior parameter error covariance matrix, \mathbf{A} , can be approximated to the inverse Hessian of the cost function, using the linearity assumption at the minimum of $J(\mathbf{x})$. It can be

1 derived with the Jacobian of the model at the end of the minimization (i.e. the last iteration),
2 \mathbf{H}_∞ , following Tarantola (1987):

$$3 \quad \mathbf{A} = [\mathbf{H}_\infty^T \cdot \mathbf{R}^{-1} \cdot \mathbf{H}_\infty + \mathbf{B}^{-1}]^{-1} \quad (4)$$

4 Note that for step 3, $\mathbf{H}_\infty = \mathbf{T} \cdot \mathbf{S}_\infty$, where \mathbf{S}_∞ is the Jacobian of the ORCHIDEE model at the
5 last iteration. The posterior parameter error covariance, \mathbf{A} , can then be propagated into the
6 model state variable space (e.g. carbon fluxes and stocks), \mathbf{A}_{var} , given the following matrix
7 product (only used for the global fluxes in step 3):

$$8 \quad \mathbf{A}_{\text{var}} = \mathbf{S}_\infty \cdot \mathbf{A} \cdot \mathbf{S}_\infty^T \quad (5)$$

9 The square root of the diagonal elements of \mathbf{A}_{var} corresponds to the standard deviation, σ , of
10 carbon fluxes/stocks for each grid cell. In order to evaluate the knowledge improvement
11 brought by the assimilation, the uncertainty reduction between the prior (σ_{prior}) and posterior
12 (σ_{post}) is determined as $1 - (\sigma_{\text{post}} / \sigma_{\text{prior}})$.

13 2.4.4 Additional processing steps

14 In order to analyze the fit to the atmospheric CO₂ concentrations in terms of the trend and
15 seasonal cycle, we decomposed the observed and modeled time series by fitting the monthly
16 mean values with a function comprising a first order polynomial term and four harmonics,
17 and then filtered the residuals of that function in frequency space using a low pass filter
18 (cutoff frequency of 65 days), following Thoning et al. (1989). The polynomial term defines
19 the trend while the seasonal cycle corresponds to the harmonics plus the filtered residuals.
20 The amplitude of the seasonal cycle is then calculated as the difference between the monthly
21 mean maximum and minimum for year 2003 (middle year of the optimization period).
22 Finally, we define the Carbon Uptake Period (CUP) as the sum of the days when the values of
23 the seasonal cycle extracted from the CO₂ concentration time series are negative (a negative
24 convention being for CO₂ removed from the atmosphere).

25 2.5 Prescribed emissions of carbon fluxes

26 In this section we describe the other components of the carbon cycle (apart from the surface C
27 exchange with terrestrial vegetation) that are imposed in step 3 of the optimization process as
28 fixed fluxes.

2.5.1 Ocean fluxes

The ocean contributes to an uptake of about a quarter to a third of the anthropogenic emissions with significant year-to-year variations (Sabine et al., 2004). For this version of the ORCHIDAS, we developed a statistical model to estimate the spatial and temporal variations (monthly) of the ocean surface CO₂ partial pressure (pCO_2^{SW}), and from that the air-sea CO₂ fluxes, using satellite and in-situ ocean measurements and model outputs. The air-sea CO₂ fluxes are primarily controlled by the ocean biogeochemistry, the horizontal transport and the vertical mixing in the ocean and the atmospheric forcing (CO₂ partial pressure at the interface to the water (pCO_2^{ATM}) and wind); they can be defined from the following equation:

$$F_{CO_2} = K_{ex} \times (pCO_2^{SW} - pCO_2^{ATM}) \quad (6)$$

where K_{ex} stands for the exchange coefficient and F_{CO_2} the CO₂ flux from the sea surface water to the atmosphere.

The computation of pCO_2^{SW} is performed using feedforward artificial neural networks, i.e., a MultiLayer Perceptron (MLP; Rosenblatt 1958) that maps a set of spatio-temporal variables (input) onto observed pCO_2^{SW} data. We use a two-step approach: the first step to derive a monthly mean pCO_2^{SW} climatology and the second step to correct for the year to year variations. The pCO_2^{SW} observations come from the Global Surface pCO₂ (Lamont-Doherty Earth Observatory, LDEO) Database (Takahashi et al., 2009). The inputs are a series of variables connected to the spatial and temporal evolution of pCO_2^{SW} : i) sea surface temperature (SST), sea surface salinity (SSS) and mixed layer depth (MLD) as a proxy of the physical processes (these fields come from a re-analysis of the NEMO-OPA ocean model (Madec et al., 1998) with the assimilation of several satellite observations), ii) chlorophyll content from SeaWiFS, as a proxy of the biogeochemistry (CHL), iii) spatial and temporal coordinates (LAT, LON and MONTH) and the pCO_2^{SW} at previous time step (recursive approach), i.e.:

$$\{pCO_2^{SW}\}_m = MLP(\{SST, SSS, MLD, CHL\}_{(m-2, m-1, m)}, \{pCO_2^{SW}\}_{(m-2, m-1)}, LAT, LON) \quad (7)$$

with m the monthly index. The available data (20685 points) is divided into two parts: 75% is used for the learning phase of the ANN and 25% for the validation phase. The overall performance of the neural network for extrapolating the spatial and seasonal distribution of pCO_2^{SW} is relatively good, with a spatio-temporal correlation coefficient between the estimated pCO_2^{SW} and the independent observations of 0.80.

$p\text{CO}_2^{\text{ATM}}$ at the surface are taken from a global simulation of atmospheric CO_2 concentrations with optimized fluxes (Chevallier et al. 2010). K_{ex} is defined as the product of k , the gas transfer velocity, taken from the Wanninkhof (1992) formulation using winds from ERA-Interim, and s , the solubility of CO_2 , taken from the Weiss formulation (Weiss, 1974). The system is further described in Roedenbeck et al. (2015). The global ocean sink is around 1.60 PgC.yr^{-1} for the period 2002-2004 used in step 3. It is within the uncertainty range of the Global Carbon Project estimates (Le Quéré et al., 2015) if we account for the pre-industrial ocean outgazing flux included in our “delta $p\text{CO}_2$ ” approach. Its temporal evolution is depicted in Fig. A1

2.5.2 Global fossil fuel and cement CO_2 emissions

We have used a recently developed CO_2 fossil fuel and cement emission product (see <http://www.carbones.eu/wcmqs/>) that covers the period 1980 to 2009 at the spatial resolution of $1^\circ \times 1^\circ$ and hourly resolution. It is based on EDGAR v4.2 spatially distributed annual emissions (Olivier et al., 2012) and time profiles developed by the University of Stuttgart (<http://carbones.ier.uni-stuttgart.de/wms/impressum.html>). It was assumed that EDGAR delivers the most up-to-date spatially distributed and sector specific emissions, based on national emission statistics. The IER (Institut für Energiewirtschaft und Rationelle Energieanwendung) further applied country and sector specific time profiles, taking into account monthly, daily, and hourly variations depending on the sector. The derivation of the time profiles relies on different data sets (e.g. Eurostat, ENSTO-E (<https://www.entsoe.eu/about-entso-e/Pages/default.aspx>), UN monthly bulletin) as well as correlations between recorded emissions and climate variables. Currently, the temporal profiles are derived mostly from data sets over Europe that were extrapolated using information on climate zone, average monthly temperature for the seasonal cycles and similarity in socio-economic parameters like population and Gross Domestic Product (GDP). The annual mean emission for the period 2002-2004 is 7.14 PgC.yr^{-1} .

2.5.3 Fire emissions:

Fire emissions data from the Global Fire Data (GFEDv3 – <http://www.globalfiredata.org/Data/index.html>) are prescribed in the ORCHIDAS (except during the model spin-up). The GFEDv3 data are broken-down into 6 sectors (deforestation, peat fires, savanna fires, agriculture, forest fires, and woodland) that are further grouped into

3 main types. We generated fluxes of CO₂ relevant for typical "burning - regrowth" processes, as detailed in Appendix A2. The first type corresponds to deforestation and peat fires with carbon permanently lost to the atmosphere, the second to agriculture and savannah fires which are assumed to be compensated by a sink during the regrowth period (i.e. with zero annual net emission for each pixel) and the third to woodland and burnt forests which are assumed to be at steady state for a given region (10 sub-continental scale regions) over the period covered by GFEDv2 (i.e. regrowth of nearby forest compensates for the burned forest derived in GFED). The sum of these three components leads to the global flux, with a gross emission around 2.1 PgC.yr⁻¹ and a net emission after regrowth of only 1.1 PgC.yr⁻¹ (Fig. A2 in Appendix) that is prescribed to the ORCHIDAS over the period 2002-2004.

3 Results

3.1 Model fit to the data

3.1.1 Step 1: assimilation of MODIS NDVI data

The optimization in Step 1 resulted in an improved fit to the MODIS NDVI observations for the four PFTs considered (TeBD, BoND, BoBD, NC3, see §2.4) as seen in Fig. 4, which shows the mean seasonal cycle across the 2000-2008 period for all sites for each PFT. The most prominent change after the optimization was a substantially shorter growing season for all PFTs due to an earlier start of leaf senescence. This was caused by both a lower critical leaf age ($L_{agecrit}$) and a higher temperature threshold for senescence (CT_{senes}) (see Fig. 9). The impact on the start of leaf growth was less dramatic but important nonetheless, with a shift to a later start of leaf growth as a result of an increase in the $K_{pheno,crit}$ parameter which acts as a scalar on the threshold of Growing Degree Days (GDD) used to trigger leaf onset (see Appendix A in MacBean et al., 2015). Overall, a mean reduction in RMSE of 23, 17, 58 and 19% was achieved for TeBD, BoBD, BoND trees and NC3 grasses respectively, with the greatest improvement for BoND trees. The mean correlation between the normalized MODIS-NDVI and modeled FAPAR time series over the 2000 – 2008 period increased for TeBD and BoND trees and NC3 grasses (prior and posterior of 0.9 to 0.93, 0.42 to 0.91 and 0.6 to 0.66, respectively). The prior correlation of 0.55 remained similar after the assimilation for BoBD trees.

1 Following the improvement at the sites selected for the optimization, we evaluated the impact
2 for each PFT at the global scale using the global median correlation between the MODIS-
3 NDVI and the model FAPAR time series (from all pixels where the fraction of a given PFT is
4 above 60%, see Maignan et al. 2011). The global correlation increased for BoND trees and
5 NC3 grasses from 0.36 to 0.91 and 0.53 to 0.59 (prior to posterior), respectively. It remains
6 stable for BoBD (0.54) or slightly increased for TeBD (0.88 to 0.89).

7 3.1.2 Step 2: assimilation of FLUXNET data

8 The optimization in Step 2 brings an improvement to the simulated NEE and LE for all seven
9 PFTs considered, with Fig. 5 showing the corresponding PFT-averaged mean NEE seasonal
10 cycles (mean across all sites/years). NEE is overestimated by the prior model for all PFTs on
11 average. This is partly due to the model spin-up procedure, which brings each simulated site
12 to a near equilibrium state with a mean NEE close to zero (i.e. no net carbon sink, see §2.1.1).
13 This bias is significantly corrected by the optimization to match the observed carbon uptake at
14 most sites, notably via the scaling of the initial soil carbon pool content at each site
15 (parameters $K_{soilC,site}$; Table 1) which thus significantly reduces the ecosystem respiration
16 (Kuppel et al., 2014). Overall, the largest reductions of model-data RMSE are found in
17 temperate forests (TeNE, TeBE and TeBD), where the RMSE decreased by more than 25%
18 compared with the prior model. The improvements are less significant for the other PFTs,
19 with RMSE reductions between 10 and 18%.

20 In addition, the optimization increases the NEE seasonal amplitude in temperate evergreen
21 forests (TeNE and TeBE) and temperate broadleaf deciduous forests (TeBD), and reduces the
22 amplitude for boreal needle leaf forest (BoNE) and natural C3 grasses (NC3), in agreement
23 with the observations (except for BoNE where the amplitude decrease is too large). Despite
24 the better model-data agreement for evergreen broadleaf forests (TrBE and TeBE), the
25 optimized model still fails to catch some seasonal features such as a persistent carbon uptake
26 (i.e. negative NEE) in the dry season for the tropical regions (TrBE) and nearly-null carbon
27 exchange in the first months of the year for temperate regions (TeBE). These results are
28 discussed further in Kuppel et al. (2014), who used a similar optimization set-up with a
29 slightly different parameter set – see §2.3.3. Similar improvements, although of smaller
30 amplitude, occur for the latent heat fluxes (not shown).

3.1.3 Step 3: assimilation of atmospheric CO₂ data

The final optimization step with the atmospheric CO₂ concentrations provides a large improvement of the fit to the observed concentrations at most stations. The cost function J was reduced through the minimization by a factor of 5.7 within 37 iterations.

Figure 6 illustrates the simulated concentrations for four stations (representative of different conditions), over the assimilation period, with the standard prior parameter vector (used in step 1), the posterior vector from step 2 (used as prior in step 3) and the posterior vector from this last step. The improvement in the fit to the observations can be quantified with the reduction in RMSE (from the prior to the posterior of step 3) - the largest reduction is at the South Pole station (73%) and is on average around 25% across all sites. Note that for a few stations the fit is slightly degraded (up to 10%) except for one Pacific site (regular ship measurements around the equator, POCN00) for which there is a 40% degradation, possibly due to small biases in the simulation of the ITCZ position in LMDz. When calculated with respect to the standard prior (used in step 1) the RMSE decrease is slightly larger on average, especially for the northern mid to high latitude stations. For these stations the optimization performed in step 2 with FLUXNET data led to a significant improvement of the mean seasonal cycle amplitude of the atmospheric CO₂ data, as discussed in Kuppel et al. (2014).

We then investigated the fit to the observed CO₂ concentrations in terms of the mean seasonal cycle and trend (see section 2.4.4). With only three years of data the mean trend is more difficult to define as it varies between stations; however, the optimization in step 3 increases the net land carbon sink in order to match the observed trend at most stations (as expected). If we take the Mauna Loa and South Pole stations that are representative of an integration of the fluxes at hemispheric scales, the prior CO₂ trend of 2.8 and 2.9 ppm.yr⁻¹ respectively, is reduced to 2.1 and 2.2 ppm.yr⁻¹ close to the observations (2.1 ppm.yr⁻¹ for both). The left panel of Fig. 7 illustrates changes in the amplitude of the simulated seasonal cycle at each station (see definition in §2.4.4). The values correspond to relative changes between the prior (of step 3) and posterior of the absolute difference between observed and modeled amplitude ($(|\Delta A_{post}| - |\Delta A_{prior}|)/|\Delta A_{prior}|$). They reveal an improvement in the seasonal cycle amplitude at nearly all stations of the southern hemisphere ($\approx 40\%$ improvement) and at the majority of the northern hemisphere stations ($\approx 15\%$). A few stations in north East Asia (3) and northwest America (4) show a small degradation of the amplitude ($\approx 15\%$). The right panel of Fig. 7 displays the changes of the Carbon Uptake Period (CUP, see §2.4.4) expressed

in terms of relative changes between prior and posterior of the absolute values of model-data differences, as for the amplitude. Most stations reveal an improvement of the CUP of around 20%, which is slightly lower than the improvement for the seasonal cycle amplitude.

Finally, we verified that the improvement is not only valid at the optimization sites but also at independent atmospheric CO₂ stations (see section 2.2.3). On average the mean RMSE for the 24 additional sites is 10.5 ppm for the prior of step 1 (prior of ORCHIDEE), 2.8 ppm for the prior or step 3 (i.e. posterior of step 2) and 2.1 ppm for the posterior of step 3. The corresponding values for the 53 sites used for the optimization are 10.5, 2.45 and 1.8 ppm, respectively. The error reduction during step 3 is thus similar for both the assimilated and the validation data sets, further confirming that the optimization provides a global improvement of the simulated carbon fluxes.

3.2 Consistency of the step-wise optimization

The main issue with a step-wise data assimilation system (versus a simultaneous approach) concerns the potential degradation of the model – data fit for the different data streams that are assimilated in previous steps. We noted that CO₂ concentrations were already improved when NDVI and FLUXNET data are assimilated (see §3.1.3), but we need to check if the final parameter set from step 3 leads to a degradation of the fit to MODIS-NDVI (step 1) and to FLUXNET (step 2) data compared to the fit achieved during the respective steps and, in the case of a significant degradation, if we still have an improvement for these data streams compared to the initial *a priori* fit.

Figure 8 summarizes the performance of the model data fit for MODIS-NDVI and FLUXNET-NEE data streams for the prior and posterior of each step by evaluating the median RMSE between the model and the observations across all sites. The values are calculated for each PFT separately. In this section, we keep in mind the fact that we do not optimize the same PFTs with FLUXNET data and with MODIS-NDVI.

Consistency for MODIS-NDVI

First, we notice again the significant RMSE reduction between the prior and step 1, as discussed in section 3.1. The fit to MODIS-NDVI (normalized data) for step 2 and step 3 shows only a significant degradation (increased RMSE) for temperate broadleaf deciduous forest (TeBD), which decreases the improvement achieved in step 1 (compared to the prior) by a factor of two. A marginal degradation for natural C3 grassland (NC3) is obtained after step 3: the RMSE increases slightly from 0.24 to 0.26, but is still lower than the prior value of

0.3. There is no degradation for boreal needleleaf deciduous trees (BoND), but a surprising small decrease of the RMSE (i.e. improvement in the model-data fit) for boreal broadleaf deciduous forests (BoBD; from 0.26 to 0.23). In this latter case, the use of additional parameters in steps 2 and 3 (see §2.4) allows further improvement of the fit between the normalized FAPAR and NDVI time series. On average the degradation of the fit to NDVI is thus very limited in step 2 and step 3, and in no case is the RMSE worse than the prior.

Consistency for FLUXNET data

Figure 8 again reveals the significant reduction of the RMSEs for NEE in step 2 compared to the standard prior or to the posterior of step 1 for most PFTs, except BoNE. We see only small degradations (increases) in RMSE between step 2 and step 3 for temperate needle leaf evergreen forests (TeNE: from 1.06 to 1.13 $\text{gC.m}^2.\text{d}^{-1}$), temperate broadleaf evergreen forests (TeBE: from 1.06 to 1.09 $\text{gC.m}^2.\text{d}^{-1}$), temperate broadleaf deciduous forests (TeBD: from 1.06 to 1.13 $\text{gC.m}^2.\text{d}^{-1}$) and boreal needle leaf evergreen forests (BoNE: from 0.59 to 0.60 $\text{gC.m}^2.\text{d}^{-1}$). An interesting feature to notice is that the NEE RMSE increases from the prior to the posterior of step 1 (i.e. before NEE has been used in the optimization in step 2). Using remote sensing products of vegetation activity or “greenness” (e.g. NDVI) to calibrate the phenology of ORCHIDEE thus does not always improve the simulated NEE, as they only provide a strong constraint on the timing of the [leaf phenology \(and thus indirectly the GPP\)](#) and a weak constraint on the maximum GPP but no constraint on the respiration fluxes. These reasons were discussed in Bacour et al. (2015) who used the same LSM and assimilation system. Overall, the reduction of the improvement of the model data fit to the NEE (step 3 versus step 2) is marginal (limited to a few percent), thus further suggesting the consistency of our step-wise approach. Similar results are also obtained for the latent heat flux (LE) (not shown).

3.3 Estimated parameter values

We now discuss the parameter values, focusing on the changes obtained through the successive steps. Figure 9 presents the prior and posterior values for each parameter together with their associated uncertainties (estimated through Eq. (4)) and the allowed range of variation. Note that nine parameters are PFT-dependent while four are global (non PFT-dependent). For the global non PFT-dependent parameters included in the step 2 optimization, we took the mean value and error-variance (see §2.4) as the prior for step 3. Note finally that

1 the parameters linked to the initial soil carbon pools ($K_{soilC,site}$, $K_{soilC,reg}$) are not shown in Fig.
2 9 as they are too numerous (though see Fig. A2 for the regional values).

3 If we first consider the phenology parameters optimized in step 1 ($K_{lai,happy}$, $K_{pheno,crit}$, L_{age_crit} ,
4 $C_{T,senes}$; see Table 1) we see that for most PFTs they do not change significantly between step
5 1 and step 3, although they differ significantly from the prior. There are few exceptions,
6 including $K_{pheno,crit}$ (the threshold for the start of the growing season) for Boreal Needleleaf
7 deciduous forests and $K_{lai,happy}$ (level of carbohydrate use) for temperate and boreal broadleaf
8 deciduous forests (TeBD, BoBD). Note that a few phenology parameters hit one of the
9 physical bounds, which may indicate model structural errors or model parameter equifinality.
10 For most phenology parameters, the uncertainties are strongly reduced during their first
11 optimization (step 1), except for a few cases like $C_{T,senes}$ for C3 grassland. Note finally that a
12 more in depth spatio-temporal validation demonstrated the generality of the optimized
13 phenology parameters across multiple sites (for further details see MacBean et al., 2015).

14 For the photosynthesis parameters (V_{cmax} , $G_{s,slope}$, C_{Topt} , SLA , f_{stress} ; see Table 1), we find a
15 similar result with little changes between step 2 and step 3, but still a significant departure
16 from the prior values. Most parameters are well constrained by the inversion, with posterior
17 uncertainties that are greatly reduced compared to the prior, except for Tropical broadleaf
18 rain-green forest (TrBR) and Boreal needle-leaf deciduous forest (BoND) for which there is
19 nearly no constraint on $G_{s,slope}$, and f_{stress} (see Table 1).

20 The non-PFT dependent respiration-related parameters ($HR_{H,c}$, Q_{10} , MR_b) mostly change in
21 step 2 and only slightly in step 3 (with an additional reduction of the error) in order to fit the
22 large-scale constraint provided by the atmospheric observations. The values of the scalar of
23 the initial soil carbon pools size for the FLUXNET site optimizations ($K_{soilC,site}$, one parameter
24 per site, not shown) were largely reduced on average, in order to decrease the heterotrophic
25 respiration (see Kuppel et al. (2014) for additional discussion). In step 3 the same scalars that
26 were defined for an ensemble of large regions ($K_{soilC,reg}$) have decreased in the southern
27 hemisphere (less than 10%; see Fig. A2 in Appendix A3) and slightly increased in the
28 northern hemisphere (around 1%), to achieve a better match to the atmospheric CO₂ growth
29 rate and north-south gradient. Importantly, we notice that for step 3, the fit to the atmospheric
30 CO₂ concentrations (especially to the trend) is achieved mainly by small changes in $K_{soilC,reg}$
31 and in few other respiration-related parameters. Note finally that the parameter controlling the
32 albedo ($K_{albedo,veg}$), modified with the FLUXNET observations only (see §2.4), is not well

1 constrained by the optimization (only a small reduction in uncertainty). Overall, most
2 parameters appear to be well constrained when first optimized, with only small changes in the
3 following steps. This suggests that the targeting of different parameter subspaces in the
4 various optimisation steps was well-chosen.

5 **3.4 Estimated carbon fluxes and uncertainties**

6 The main objective of a carbon cycle data assimilation procedure is to improve the simulated
7 land surface net and gross carbon fluxes as well as the simulated carbon stocks for both
8 present and future conditions. Given the focus of the paper, i.e. to describe the potential of a
9 step-wise global carbon cycle data assimilation system, we only discuss a few large-scale
10 features of the optimized annual net and gross carbon fluxes, as well as one of the carbon
11 stock variables (forest above-ground biomass). We thus do not discuss the inter-annual flux
12 variability.

13 **Large-scale annual mean net fluxes**

14 The mean annual carbon fluxes (NEE) for the globe, northern extra tropics, tropics, and
15 southern extra tropics are reported in Fig. 10 for the 2000-2009 decade for the prior and
16 posterior model simulations for all steps. We ran the optimized model over the full 2000's
17 decade in order to compare with one other estimate of the land surface residual from the
18 Global Carbon Project (GCP, Le Quéré et al, 2015) over the same decade. The prior NEE
19 indicates a total sink of 0.5 PgC.yr⁻¹ over this period, from both the northern and tropical
20 regions. Such a prior sink is due to the increase of atmospheric CO₂ during the transient
21 simulation following the spin-up (1990-2009, see section 2.3.1) and climate variability.
22 Changes from the prior are rather small in step 1 (assimilation of MODIS NDVI)) with an
23 increase of the northern sink by 0.12 PgC.yr⁻¹ and a decrease of the tropical sink by 0.05
24 PgC.yr⁻¹ (Fig. 10). Step 2 (assimilation of FLUXNET data) does not significantly change the
25 net C sink from step 1, with only a small increase in the tropical sink by 0.1 PgC.yr⁻¹. The
26 assimilation of atmospheric CO₂ data in step 3 provides a large-scale constraint, as already
27 discussed, and increases the total land sink to 2.2 PgC.yr⁻¹, a value in much closer agreement
28 with the estimate by the GCP. A larger tropical NEE uptake is responsible for the large
29 increase of the terrestrial biosphere C sink (from 0.3 PgC.yr⁻¹ in step 2 to 1.7 PgC.yr⁻¹) while
30 the sink in the north increases by less than 0.1 PgC.yr⁻¹. The comparison with the GCP
31 number should be taken with caution. The ORCHIDAS estimated sink include all effects

Philippe Peylin 15/8/16 23:31
Supprimé: together

(natural and anthropogenic), since that we used atmospheric CO₂ as a global constraint. Thus the optimized parameters must account for any missing processes like nitrogen limitation or a proper description of agricultural processes and management. However, the GCP number is only for the anthropogenic uptake, excluding the pre-industrial sink due for instance to river export of carbon (around 0.45 PgC.yr⁻¹; Regnier et al. 2013).

Spatial distribution of the annual mean net flux

Figure 11 shows the spatial distribution of NEE averaged over 2002-2004 for the standard prior and posterior after step 3. The large tropical net land carbon sink that is inferred in step 3 is mainly explained by an increase of the carbon uptake for the tropical forests of the Amazon basin and equatorial Africa, as well as a decrease of the carbon release on the southern edge of the Amazon basin (tropical rain-green forests and grasses). In the northern mid-high latitudes only smaller regional changes from the prior occur. For Europe, most of north Asia and Canada, the strength of the C sink slightly decreased from the prior (up to 30 gC.m².yr⁻¹), while for central USA the strength of C source slightly decreased. If we now consider the uncertainties on the net annual carbon flux that arise from the parameter uncertainty (second row of Fig. 10; Eq. (5)) we observe a very large reduction (compared to the prior) in the monthly flux uncertainty (averaged over the three years used in step 3) over tropical forests. It is reduced by a factor four with initial values around 150 gC.m².y⁻¹ and posterior values between 22 and 66 gC.m².y⁻¹. For mid-to-high latitude boreal ecosystems, the uncertainty reduction is smaller, but the posterior errors are slightly lower than over the tropics, between 18 and 55 gC.m².y⁻¹.

Large-scale annual mean Gross Primary Production (GPP)

For the GPP the relative changes from the prior are smaller than for the NEE (Fig. 10b). The mean annual total GPP is 172, 155, 156 and 157 PgC.yr⁻¹ for the prior and posterior of step 1, 2 and 3, respectively. The small overall decrease (9%) brings the GPP slightly closer to the estimate by Jung et al. (2011), around 120 PgC.yr⁻¹, based on a statistical Model Tree Ensemble (MTE) that upscaled the in-situ flux measurements (resulting from the partition of measured NEE into GPP and total ecosystem respiration). The decrease in GPP occurs mainly in the northern hemisphere after step 1 (-10 PgC.yr⁻¹) following the decrease in V_{cmax} (Fig. 9) while it remains relatively stable over the tropics across all steps. Note that i) the study of Welp et al. (2011) suggests a GPP around 150 PgC.yr⁻¹, similar to our estimate, based on

measurements of $^{18}\text{O}/^{16}\text{O}$ ratio in atmospheric CO_2 and ii) Koffi et al. (2012) found optimized GPP of 146 PgC.yr^{-1} from a CCDAS using the BETHY model.

Above-ground forest biomass

We analyze the impact of the optimization on the forest above-ground biomass at equilibrium (i.e. after spin-up; see Fig. 12) as an example of the impact on model C stocks, and compare the simulated values, for the same three latitude bands than above, to the estimate based on field observations and remote sensing data. This product, which was produced in the GEOCARBON project (and thus is referred to by the same name), integrates a pan-tropical biomass map (Avitabile et al., 2015) with a boreal forest biomass product (Santoro et al., 2015).

For the northern extra tropics, the prior above-ground C stock ($\sim 180 \text{ PgC}$) is reduced by the optimization to 140 PgC , mainly through the decrease of the growing season length in step 1 with the assimilation of MODIS-NDVI. The significant decrease in GPP during step 1 (18 %) led indeed to a similar decrease of the forest biomass (16%). Parameter changes through the assimilation of FLUXNET and CO_2 data have a smaller impact (a change of less than 5 PgC). These changes in the northern extra tropics bring the estimates by the ORCHIDEE model closer to the satellite-based GEOCARBON product ($\sim 120 \text{ PgC}$).

For the tropics, while there is nearly no change with the assimilation of MODIS-NDVI in step 1, the use of FLUXNET data leads to a significant increase of the forest above ground biomass (close to 25%). Such an increase does not correspond to an increase of the GPP (Fig. 10) but to changes in the autotrophic respiration parameter (MR_b) that lead to a decrease of autotrophic respiration and an increase of NPP. The value does not change through step 3 and remains significantly higher than the data-driven estimate. Note however that the lower value in the GEOCARBON product could be partly due to the fact that we did not yet account for land use effects in the CCDAS, such as deforestation in the Amazon.

4 Discussion and conclusions

In this paper we have described a first global Carbon Cycle Data Assimilation System that assimilates three major carbon-cycle related data streams, namely MODIS-NDVI observations of vegetation activity at 60 sites, FLUXNET NEE and LE measurements at more than 70 sites, and atmospheric CO_2 concentrations at 53 surface stations over three years in

1 order to optimize the C cycle parameters of the ORCHIDEE process-based LSM
2 (ORCHIDEE-CCDAS). The study details the concept, the implementation and the main
3 results of a stepwise assimilation approach where the data streams have been assimilated in
4 three successive steps (including a propagation of the retrieved posterior parameter
5 distributions from one step to the next).

6 The assimilation of MODIS-NDVI (60 grid cell points, step 1) improved the phenology of
7 ORCHIDEE with a significant reduction of the growing season length and thus a direct
8 impact on the GPP. The results are similar to those presented in MacBean et al. (2015) who
9 describe the impact of such optimization on the global FAPAR simulations and the
10 improvement in the bias of the calculated leaf onset and senescence dates in more detail. The
11 optimization with FLUXNET data (78 sites, step 2) led to large improvements in the seasonal
12 cycle of the NEE and LE fluxes, constraining primarily the photosynthetic processes. Some
13 discrepancies remain due to site heterogeneity (i.e. different species and edaphic conditions)
14 that the model does not fully capture, and due to missing processes in the model (see Kuppel
15 et al. (2014) for a more thorough discussion). However, without the assimilation of
16 atmospheric CO₂ concentrations, the global (and continental) net carbon balance after step 2
17 was still clearly outside the admitted range (as reported by the GCP in Le Quéré et al. (2015),
18 which highlights the importance of assimilating a data stream such as this that provides
19 information at larger scales (constraining large scale respiration fluxes). The use of
20 atmospheric CO₂ concentration as an overall constraint in step 3 was technically challenging
21 as it required the coupling of ORCHIDEE with an atmospheric transport model in forward
22 and reverse mode (i.e. to compute the cost function and its gradients at each step of the
23 minimization process). As a result of the final step, we were able to fit the atmospheric CO₂
24 growth rate and thus to derive a land C sink compatible with current best estimates from the
25 GCP. The assimilation of CO₂ data also slightly changed the seasonality of the NEE, which
26 improved the fit to the atmospheric CO₂ seasonal cycle. Note that assimilating only CO₂ data
27 would lead to a similar global land C sink but with a different model parameter set not
28 compatible with the information provided by MODIS-NDVI and FLUXNET data.

29 The consistency of the stepwise approach has been evaluated with back-compatibility checks
30 after the final step (step 3: assimilation of atmospheric CO₂ concentration). The optimized
31 model with the final set of parameters does not degrade the fit to MODIS-NDVI and
32 FLUXNET data that were assimilated in the first two steps (only minor changes of the

1 RMSEs occur; see Fig. 8). This result has two important consequences. Most importantly it
 2 suggests that current state of the art LSMs (at least ORCHIDEE) have reached a level of
 3 development where consistent assimilation of multiple data streams is finally possible. This
 4 overcomes the most important limitation noted by Rayner (2010) to the widespread use of
 5 CCDAS systems. At a more technical level it suggests that stepwise assimilation is a valid
 6 and feasible approach. Although we only carried the estimated parameter uncertainties from
 7 one step to the next (as a first more simple approach), and not the full error variance-
 8 covariance matrix, we were able to propagate enough information to maintain an optimal
 9 model-data fit after the last step for the three data streams, as confirmed with the back-
 10 compatibility checks. MacBean et al. (2016) provide a more specific analysis of this issue.
 11 However, not propagating the covariance terms may have a larger impact for the reduction of
 12 the inferred parameter uncertainties (see for instance the large parameter / flux error reduction
 13 in Fig. 9 / Fig. 11). The order of the different steps was dictated by the number of parameters
 14 we choose to expose to each data stream, from only a few phenology parameters for NDVI up
 15 to the largest set for atmospheric CO₂. Recall that under the fundamental theory the order of
 16 assimilation is unimportant. Testing whether our system meets this criterion is an important
 17 check on the robustness of the method but is not technically feasible with the full-blown
 18 system; it is currently being tested with some smaller models.

19 Most of the optimized parameter values have significantly changed compared to their prior
 20 values, with a large error reduction for most (Fig. 9) that results in a strong constraint on the
 21 simulated fluxes (Fig. 11). In the last step, the assimilation of atmospheric CO₂ data mainly
 22 led to the optimization of respiration-related parameters, especially the regional soil carbon
 23 multipliers ($K_{soilC,reg}$). Note that this was also the case for the BETHY-CCDAS, as described
 24 in Rayner et al. (2005) (see their Table 2). This is linked to the difficult issue of representing
 25 the effects of historical changes in land cover and land management as well as soil texture
 26 effects on soil carbon dynamics, and the necessary choice of a standard spin-up procedure to
 27 account for these effects. Ideally one would need to perform the optimization of the model
 28 over a long historical period with LULCC and land management practices included and the
 29 optimization of related parameters. However, this is not currently feasible at global scale and
 30 uncertainties in the forcing would introduce as much difficulty as uncertainties in the initial
 31 condition. The adjustment of the initial C pool contents is thus a logical compromise and
 32 further investigations into the impact of the selected set-up (number of regions for $K_{soilC,reg}$,
 33 their associated uncertainties) on the C fluxes simulated in the future are needed. Note that a

first improvement would be to include LULCC in the transient simulation (to define the initial state) before the assimilation period.

Nonetheless, several limitations, inherent to the optimization of model parameters in a CCDAS, need to be called to mind when evaluating these results (see also Rayner et al., 2010). First, the structure of the land surface model (i.e. how biogeochemical processes are represented) is critical. Any missing/misrepresented processes may have a direct impact and thus lead to biases in the selected parameters. Note that this limitation could be even more severe when using atmospheric CO₂ measurements, as these data provide a direct constraint on the overall net C exchange between the atmosphere and the vegetation, thus including all processes. As an example, the model sensitivity to atmospheric CO₂ increase (e.g. through the parameters V_{max} and $G_{s,slope}$) could be non optimal as the current model version does not include explicit nitrogen and phosphorus limitations on photosynthesis. Second, the chosen set of observations does not provide specific constraints on long term C processes such as tree mortality, disturbance effects, or C allocation within a plant. For instance Fig. 12 illustrates that the optimized model may still significantly overestimate tropical forest biomass. The assimilation of above-ground biomass or soil carbon stock observations (i.e. site-level measurements or regional estimates) should thus provide critical complementary information (see Bloom et al., 2016 and Thum et al., in revision for AFM). Additionally, uncertainties on the other components of the carbon cycle, such as fossil fuel and biomass burning emissions and ocean fluxes, can be also critical when using atmospheric CO₂ as a constraint. Finally, one can mention new approaches based on remote sensing data to account for site level differences in productivity potential due to edaphic variability (soil quality and slope/drainage) within the same vegetation type, as illustrated for high latitudes in North America (Ise and Sato, 2008).

To conclude, this work is a step forward in terms of multiple data streams assimilation that opens new perspectives for a better understanding of the carbon cycle and better predictions of the fate of the land carbon sink in the 21st century as a consequence of anthropogenic changes. As ORCHIDEE is part of the IPSL earth system model the impact of the optimization on future climate change predictions will be assessed in a future study. However, we first need to run the ORCHIDAS with a longer atmospheric CO₂ record (i.e. several decades) in order to provide stronger constraints on parameters controlling the impact of climate extremes on the net carbon fluxes at continental to global scales, and the sensitivity of

1 photosynthesis to increasing CO₂ concentration. The optimized model will allow a more in-
2 depth investigation of the trend and inter-annual variations of land surface C fluxes at
3 continental to regional scales, as well as their driving mechanisms. It will offer a more
4 reliable and robust process-based diagnostic of the land C cycle that is compatible with
5 current major data streams. Overall, we have illustrated the benefit of combining multiple
6 data streams in a process-based model to optimize different processes of the model, related to
7 different temporal and spatial scales. The optimization will be updated regularly as new
8 processes are integrated into the ORCHIDEE model, such as for instance land management
9 (Naudts et al., 2015).

11 **Code availability**

12 The ORCHIDEE model code and the run environment are open source
13 (<http://forge.ipsl.jussieu.fr/orchidee>) and the associated documentation can be found at
14 <https://forge.ipsl.jussieu.fr/orchidee/wiki/Documentation>. Note that the tangent linear version
15 of the ORCHIDEE model has been generated using commercial software (TAF;
16 <http://www.fastopt.com/products/taf/taf.shtml>). For this reason, only the “forward” version of
17 the ORCHIDEE model is available for sharing. The optimization scheme (in Python) is
18 available through a dedicated web site for data assimilation with ORCHIDEE
19 (<http://orchidas.lsce.ipsl.fr/>). Nevertheless readers interested in running ORCHIDEE are
20 encouraged to contact the corresponding author for full details and latest bug fixes. Finally,
21 the source code of the LMDZ atmospheric transport model can be found at
22 <http://web.lmd.jussieu.fr/trac>.

24 **Appendix**

25 **A1. Ocean fluxes**

26 Figure A1 displays the air-sea fluxes from the statistical model.

27 **A2. Fire fluxes**

28 In order to account for fundamental differences between six fire flux categories provided by
29 the GFED product, we grouped these emissions into 3 types with specific treatments. The first

1 group includes C emissions from deforestation and peat fires, which are considered to be
2 permanent carbon lost to the atmosphere, at least over the considered time scales. These
3 fluxes are rescaled to an annual emission of 1.1 PgC.yr⁻¹ globally following typical values
4 reported in the literature for deforestation (Houghton R., 2003). The second group consists of
5 C emissions from agriculture and savannah fires, which are compensated by a C sink during
6 the regrowth of these biomes (i.e., savannah and some type of plants on the farmland). These
7 effects are not completely accounted for in ORCHIDEE as the model does not simulate
8 savannah and agriculture fire. Hence, the emissions over the whole period and for each pixel
9 become zero, but their seasonal variations are used. The final group includes emissions from
10 woodland and burnt forests. We considered that at steady state and for a given region certain
11 forests burn but that nearby forests are re-growing following older fires. We thus imposed
12 regrowth at the region scale given that the ORCHIDEE model version that we use does not
13 account for such regrowth. The main assumption is that over century time scale the
14 forest/woodland system is at steady state over a given region (few thousand square km), i.e.
15 there is no net deforestation. We selected an ensemble of small regions over which we
16 calculated the regrowth of these biomes. The derived emissions over the whole period and for
17 each region thus become zero; though we include their spatial and temporal variations. The
18 overall biomass burning flux considered in the CCDAS for the optimization process is the
19 sum of the three fluxes as described above.

20 **A3. Multipliers of the soil initial carbon pools**

21 Figure A2 provides the optimized values of the $K_{soilC,reg}$ parameters that optimize the initial
22 soil carbon pool sizes.

23 .

24 **Acknowledgements**

25 This work was mainly funded by the EU FP7 CARBONES project (contracts FP7-SPACE-
26 2009-1-242316), with also a small contribution from GEOCARBON project
27 (ENV.2011.4.1.1-1-283080). This work used eddy covariance data acquired by the
28 FLUXNET community and in particular by the following networks: AmeriFlux (U.S.
29 Department of Energy, Biological and Environmental Research, Terrestrial Carbon Program
30 (DE-FG02-04ER63917 and DE-FG02-04ER63911)), AfriFlux, AsiaFlux, CarboAfrica,
31 CarboEuropeIP, CarboItaly, CarboMont, ChinaFlux, Fluxnet-Canada (supported by CFCAS,
32 NSERC, BIOCAP, Environment Canada, and NRCan), GreenGrass, KoFlux, LBA, NECC,

1 OzFlux, TCOS-Siberia, USCCC. We acknowledge the financial support to the eddy
2 covariance data harmonization provided by CarboEuropeIP, FAO-GTOS-TCO, iLEAPS, Max
3 Planck Institute for Biogeochemistry, National Science Foundation, University of Tuscia,
4 Université Laval and Environment Canada and US Department of Energy and the database
5 development and technical support from Berkeley Water Center, Lawrence Berkeley National
6 Laboratory, Microsoft Research eScience, Oak Ridge National Laboratory, University of
7 California-Berkeley, University of Virginia. P. C. acknowledges support from the European
8 Research Council through Synergy grant ERC-2013-SyG-610028 “IMBALANCE-P ». The
9 MODIS MOD09CMG collection 5 surface reflectance data are freely available to download
10 from the Land Processes Distributed Active Archive Center (LP DAAC) data portal
11 (<https://lpdaac.usgs.gov>). The authors wish to thank M. Jung for providing access to the GPP
12 MTE data, which were downloaded from the GEOCARBON data portal ([https://www.bgc-](https://www.bgc-jena.mpg.de/geodb/projects/Data.php)
13 [jena.mpg.de/geodb/projects/Data.php](https://www.bgc-jena.mpg.de/geodb/projects/Data.php)). The authors are also grateful to computing support and
14 resources provided at LSCE and to the overall ORCHIDEE project that coordinate the
15 development of the code (<http://labex.ipsl.fr/orchidee/index.php/about-the-team>).

16
17
18
19
20
21
22
23

References

- Alton, P. B.: From site-level to global simulation: Reconciling carbon, water and energy fluxes over different spatial scales using a process-based ecophysiological land-surface model, *Agric. For. Meteorol.*, 176, 111–124, doi:10.1016/j.agrformet.2013.03.010, 2013.
- Avitabile V, Herold M, Heuvelink G, Lewis SL, Phillips OL, Asner GP et al. (2015). An integrated pan-tropical biomass maps using multiple reference datasets. *Global Change Biology*.
- Bacour, C., Peylin, P., MacBean, N., Rayner, P. J., Delage, F., Chevallier, F., Weiss, M., Demarty, J., Santaren, D., Baret, F., Berneiller, D., Dufrêne, E. and Prunet, P.: Joint assimilation of eddy covariance flux measurements and FAPAR products over temperate forests within a process-oriented biosphere model, *J. Geophys. Res. Biogeosciences*, 120, 1–19, doi:10.1002/2015JG002966, 2015.
- Bloom, A. A., Exbrayat, J.-F., van der Velde, I. R., Feng, L. and Williams, M.: The decadal state of the terrestrial carbon cycle: Global retrievals of terrestrial carbon allocation, pools, and residence times., *Proc. Natl. Acad. Sci. U. S. A.*, 113(5), 1285–1290, doi:10.1073/pnas.1515160113, 2016.
- Bousquet P., D. Hauglustaine, P. Peylin, C. Carouge, and P. Ciais, Two decades of OH variability as inferred by an inversion of atmospheric transport and chemistry of methyl chloroform, *Atmos. Chem. and Phys.*, 5, 263-2656, ISI:000232370800002, 2005.
- Braswell, B. H., Sacks, W. J., Linder, E. and Schimel, D. S.: Estimating diurnal to annual ecosystem parameters by synthesis of a carbon flux model with eddy covariance net ecosystem exchange observations, *Glob. Change Biol.*, 11(2), 335–355, doi:10.1111/j.1365-2486.2005.00897.x, 2005.
- Byrd, R. H., P. Lu, J. Nocedal, and C. Zhu (1995), A limited memory algorithm for bound constrained optimization, *SIAM J. Sci. Stat. Comput.*, 16(5), 1190–1208.
- Canadell, J. G., Ciais, P., Sabine, C., and Joos, F. (Eds.): REgional Carbon Cycle Assessment and Processes (RECCAP), Special issue, *Biogeosciences*, http://www.biogeosciences-discuss.net/special_issue83.html, 2013.
- Chevallier F., Fisher M., Peylin P., Serrar S., Bousquet P., Bréon F-M., Chédin A., Ciais P. (2005), Inferring CO2 sources and sinks from satellite observations: Method and application to TOVS data, *Journal of Geophysical Research*, **110**, D24309, doi:20.1029/2005JD006390, 13pp.
- Chevallier, F., P. Ciais, T. J. Conway, T. Aalto, B. E. Anderson, P. Bousquet, E. G. Brunke, L. Ciattaglia, Y. Esaki, M. Fröhlich, A.J. Gomez, A.J. Gomez-Pelaez, L. Haszpra, P. Krummel, R. Langenfelds, M. Leuenberger, T. Machida, F. Maignan, H. Matsueda, J. A. Morgui, H. Mukai, T. Nakazawa, P. Peylin, M. Ramonet, L. Rivier, Y. Sawa, M. Schmidt, P. Steele, S. A. Vay, A. T. Vermeulen, S. Wofsy, D. Worthy, (2010), CO2 surface fluxes at grid point scale estimated from a global 21-year reanalysis of atmospheric measurements, *Journal of Geophysical Research*, **115**, D21307, doi:10.1029/2010JD013887.

1 Collatz GJ, Ribas-Carbo M, Berry JA, (1992), Coupled Photosynthesis-Stomatal Conductance
2 Model for Leaves of C4 Plants. *Aust J Plant Physiol*, **19**: 519-38.

3 de Rosnay P, Polcher J. (1998), Modelling root water uptake in a complex land surface
4 scheme coupled to a GCM. *Hydrol Earth Syst Sc*, **2**: 239-55.

5 Dee, D. P., Uppala, S. M., Simmons, A. J., Berrisford, P., Poli, P., Kobayashi, S., Andrae, U.,
6 Balmaseda, M. A., Balsamo, G., Bauer, P., Bechtold, P., Beljaars, A. C. M., van de Berg, L.,
7 Bidlot, J., Bormann, N., Delsol, C., Dragani, R., Fuentes, M., Geer, A. J., Haimberger, L.,
8 Healy, S. B., Hersbach, H., Hólm, E. V., Isaksen, L., Kållberg, P., Köhler, M., Matricardi, M.,
9 McNally, A. P., Monge-Sanz, B. M., Morcrette, J. J., Park, B. K., Peubey, C., de Rosnay, P.,
10 Tavolato, C., Thépaut, J. N., and Vitart, F.: The ERA-interim reanalysis: configuration and
11 performance of the data assimilation system, *Q. J. Roy. Meteor. Soc.*, **137**, 553–597,
12 doi:10.1002/qj.828, 2011.

13 Ducoudre NI, Laval K, Perrier A. Sechiba (1993), A New Set of Parameterizations of the
14 Hydrologic Exchanges at the Land Atmosphere Interface within the Lmd Atmospheric
15 General-Circulation Model. *J Climate*, **6**: 248-73.

16 Dufresne, J.-L., et al. (2011), Climate change projections using the IPSL-CM5 Earth System
17 Model: from CMIP3 to CMIP5, submitted to *Clim. Dynam.*

18 Farquhar, G. D., von Caemmerer, S. von and Berry, J. A.: A biochemical model of
19 photosynthetic CO₂ assimilation in leaves of C3 species, *Planta*, **149**(1), 78–90, 1980.

20 Folberth G., Hauglustaine D.A., Ciais P., et al. (2005), On the role of atmospheric chemistry
21 in the global CO₂ budget, *Geophysical Research Letters*, **32**(8): L08801

22 Fung, I. Y., C. J. Tucker, and K. C. Prentice, Application of Advanced Very High Resolution
23 Radiometer vegetation index to study atmosphere – biosphere exchange of CO₂, *J. Geophys.*
24 *Res.*, **92**, 2999– 3015, 1987.

25 GLOBALVIEW : Cooperative Global Atmospheric Data Integration Project. 2013, updated
26 annually. Multi-laboratory compilation of synchronized and gap-filled atmospheric carbon
27 dioxide records for the period 1979-2012 (obspack_co2_1_GLOBALVIEW-
28 CO2_2013_v1.0.4_2013-12-23). Compiled by NOAA Global Monitoring Division: Boulder,
29 Colorado, U.S.A. Data product accessed at <http://dx.doi.org/10.3334/OBSPACK/1002>.

30 Groenendijk, M., Dolman, a. J., van der Molen, M. K., Leuning, R., Arneth, a., Delpierre,
31 N., Gash, J. H. C., Lindroth, a., Richardson, a. D., Verbeeck, H. and Wohlfahrt, G.:
32 Assessing parameter variability in a photosynthesis model within and between plant
33 functional types using global Fluxnet eddy covariance data, *Agric. For. Meteorol.*, **151**(1),
34 22–38, doi:10.1016/j.agrformet.2010.08.013, 2011.

35 Hauglustaine D.A., Hourdin F., Jourdain L., et al. (2004), Interactive chemistry in the
36 Laboratoire de Meteorologie Dynamique general circulation model: Description and
37 background tropospheric chemistry evaluation, *Journal of Geophysical Research -*
38 *Atmosphere*, **109**(D4): D04314

- 1 Houghton, R. A. (2003) Revised estimates of the annual net flux of carbon to the atmosphere
2 from changes in land use and land management 1850-2000. *Tellus* **55B**: 378-390.
- 3 Hourdin F. and Armengaud A. (1999), The use of finite-volume methods for atmospheric
4 advection of trace species. Part I: Test of various formulations in a general circulation
5 model, *Monthly Weather Review*, **127**(5): 822-837
- 6 Hourdin, F. et al. (2006), The LMDZ4 general circulation model: climate performance and
7 sensitivity to parametrized physics with emphasis on tropical convection, *Climate*
8 *Dynamics*, **27**(7), 787-813, 2006.
- 9 IPCC, (2007). Climate Change 2007: The Physical Science Basis. Contribution of Working
10 Group I to the Fourth Assessment Report of the Intergovernmental Panel on Climate Change
11 [Solomon, S., D. Qin, M. Manning (eds.)]
- 12 Ise, T., and H. Sato, Representing subgrid-scale edaphic heterogeneity in a largescale
13 ecosystem model: A case study in the circumpolar boreal regions, *Geophys. Res. Lett.*, **35**,
14 L20407, doi:10.1029/2008GL035701, 2008.
- 15 Kaminski, T., Knorr, W., Scholze, M., Gobron, N., Pinty, B., Giering, R. and Mathieu, P-P.
16 (2012), Consistent assimilation of MERIS FAPAR and atmospheric CO₂ into a terrestrial
17 vegetation model and interactive mission benefit analysis, *Biogeosciences*, **9**, 3173-3184.
- 18 Kaminski, T., Knorr, W., Schürmann, G., Scholze, M., Rayner, P. J., Zaehle, S., Blessing, S.,
19 Dorigo, W., Gayler, V., Giering, R., Gobron, N., Grant, J. P., Heimann, M., Hooker-Stroud,
20 a., Houweling, S., Kato, T., Kattge, J., Kelley, D., Kemp, S., Koffi, E. N., Köstler, C.,
21 Mathieu, P. P., Pinty, B., Reick, C. H., Rödenbeck, C., Schnur, R., Scipal, K., Sebal, C.,
22 Stacke, T., Van Scheltinga, a. T., Vossbeck, M., Widmann, H. and Ziehn, T.: The
23 BETHY/JSBACH Carbon Cycle Data Assimilation System: Experiences and challenges, *J.*
24 *Geophys. Res. Biogeosciences*, **118**(4), 1414–1426, doi:10.1002/jgrg.20118, 2013.
- 25 Kato, T., Knorr, W., Scholze, M., Veenendaal, E., Kaminski, T., Kattge, J. and Gobron, N.:
26 Simultaneous assimilation of satellite and eddy covariance data for improving terrestrial water
27 and carbon simulations at a semi-arid woodland site in Botswana, *Biogeosciences*, **10**(2),
28 789–802, doi:10.5194/bg-10-789-2013, 2013.
- 29 Keenan, T. F., Davidson, E. a., Munger, J. W. and Richardson, A. D.: Rate my data:
30 Quantifying the value of ecological data for the development of models of the terrestrial
31 carbon cycle, *Ecol. Appl.*, **23**(1), 273–286, doi:10.1890/12-0747.1, 2013.
- 32 Keenan, T. F., Davidson, E., Moffat, A. M., Munger, W. and Richardson, A. D.: Using
33 model-data fusion to interpret past trends, and quantify uncertainties in future projections, of
34 terrestrial ecosystem carbon cycling, *Glob. Change Biol.*, **18**(8), 2555–2569,
35 doi:10.1111/j.1365-2486.2012.02684.x, 2012.
- 36 Knorr, W. and Kattge, J.: Inversion of terrestrial ecosystem model parameter values against
37 eddy covariance measurements by Monte Carlo sampling, *Glob. Change Biol.*, **11**(8), 1333–
38 1351, doi:10.1111/j.1365-2486.2005.00977.x, 2005.

1 Knyazikhin, Y., Martonchik, J.V., Myneni, R.B., Diner, D.J., and Running, S.W. (1998),
2 Synergistic algorithm for estimating vegetation canopy leaf area index and fraction of
3 absorbed photosynthetically active radiation from MODIS and MISR, *Journal of Geophysical*
4 *Research*, **103**, D24, 32,257-32,276.

5 Koffi, E. N., Rayner, P. J., Scholze, M., & Beer, C. (2012). Atmospheric constraints on gross
6 primary productivity and net ecosystem productivity: Results from a carbon cycle data
7 assimilation system. *Global biogeochemical cycles*, 26(1).

8 Krinner, G., Viovy, N., de Noblet-Ducoudré, N., Ogée, J., Polcher, J., Friedlingstein, P.,
9 Ciais, P., Sitch, S. and Prentice, I. C.: A dynamic global vegetation model for studies of the
10 coupled atmosphere-biosphere system, *Glob. Biogeochem. Cycles*, 19(1) [online] Available
11 from: <http://onlinelibrary.wiley.com/doi/10.1029/2003GB002199/pdf> (Accessed 23
12 November 2015), 2005.

13 Kuppel, S., Chevallier, F. and Peylin, P.: Quantifying the model structural error in carbon
14 cycle data assimilation systems, *Geosci. Model Dev.*, 6(1), 45–55, doi:10.5194/gmd-6-45-
15 2013, 2013.

16 Kuppel, S., Peylin, P., Chevallier, F., Bacour, C., Maignan, F. and Richardson, A. D.:
17 Constraining a global ecosystem model with multi-site eddy-covariance data, *Biogeosciences*,
18 9(10), 3757–3776, doi:10.5194/bg-9-3757-2012, 2012.

19 Kuppel, S., Peylin, P., Maignan, F., Chevallier, F., Kiely, G., Montagnani, L. and Cescatti, A.:
20 Model–data fusion across ecosystems: from multisite optimizations to global simulations,
21 *Geosci. Model Dev.*, 7(6), 2581–2597, 2014.

22 Lasslop, G., M. Reichstein, D. Papale, A. D. Richardson, A. Arneth, A. Barr, P. Stoy, and G.
23 Wohlfahrt. 2010. Separation of net ecosystem exchange into assimilation and respiration
24 using a light response curve approach: critical issues and global evaluation. *Global Change*
25 *Biology*, **16**, 187-208.

26 Lasslop, G., M. Reichstein, J. Kattge, and D. Papale. 2008. Influences of observation errors in
27 eddy flux data on inverse model parameter estimation. *Biogeosciences*, **5**, 1311-1324.

28 Le Quéré, C., Moriarty, R., Andrew, R. M., Peters, G. P., Ciais, P., Friedlingstein, P., Jones,
29 S. D., Sitch, S., Tans, P., Arneth, a., Boden, T. a., Bopp, L., Bozec, Y., Canadell, J. G., Chini,
30 L. P., Chevallier, F., Cosca, C. E., Harris, I., Hoppema, M., Houghton, R. a., House, J. I., Jain,
31 a. K., Johannessen, T., Kato, E., Keeling, R. F., Kitidis, V., Klein Goldewijk, K., Koven, C.,
32 Landa, C. S., Landschützer, P., Lenton, a., Lima, I. D., Marland, G., Mathis, J. T., Metzl, N.,
33 Nojiri, Y., Olsen, a., Ono, T., Peng, S., Peters, W., Pfeil, B., Poulter, B., Raupach, M. R.,
34 Regnier, P., Rödenbeck, C., Saito, S., Salisbury, J. E., Schuster, U., Schwinger, J., Séférian,
35 R., Segschneider, J., Steinhoff, T., Stocker, B. D., Sutton, a. J., Takahashi, T., Tilbrook, B.,
36 van der Werf, G. R., Viovy, N., Wang, Y.-P., Wanninkhof, R., Wiltshire, a. and Zeng, N.:
37 Global carbon budget 2014, *Earth Syst. Sci. Data*, 7(1), 47–85, doi:10.5194/essd-7-47-2015,
38 2015.

- 1 Liss, P. and Merlivat, L. (1986). The role of sea-air exchange in geochemical cycling, Ed. P.
2 Menard, chapter Air-sea gas exchange rates: Introduction and synthesis, pages 113-127.
3 Reidel, Dordrecht.
- 4 MacBean, N., Maignan, F., Peylin, P., Bacour, C., François-Marie, B. and Ciais, P.: Using
5 satellite data to improve the leaf phenology of a global Terrestrial Biosphere Model,
6 *Biogeosciences*, 12, 7185-7208, 2015.
- 7 MacBean, N., Peylin, P., Chevallier, F., Scholze, M. and G. Schürmann, Consistent
8 assimilation of multiple data streams in a Carbon Cycle Data Assimilation System,
9 *Biogeosciences*, submitted, 2016.
- 10 Madec, G., P. Delecluse, M. Imbard and C. Lévy, 1998 : OPA 8.1 Ocean General Circulation
11 Model reference manual, Note du Pole de Modelisation, Institut Pierre-Simon Laplace, 11,
12 91pp.
- 13 Maignan, F., Bréon, F.-M., Chevallier, F., Viovy, N., Ciais, P., Garrec, C., Trules, J., and
14 Mancip, M.: Evaluation of a Global Vegetation Model using time series of satellite vegetation
15 indices, *Geosci. Model Dev.*, 4, 1103-1114, doi:10.5194/gmd-4-1103-2011, 2011.
- 16 Moore, D. J. P., Hu, J., Sacks, W. J., Schimel, D. S. and Monson, R. K.: Estimating
17 transpiration and the sensitivity of carbon uptake to water availability in a subalpine forest
18 using a simple ecosystem process model informed by measured net CO₂ and H₂O fluxes,
19 *Agric. For. Meteorol.*, 148(10), 1467–1477, doi:10.1016/j.agrformet.2008.04.013, 2008.
- 20 Naudts, K., Ryder, J., J McGrath, M., Otto, J., Chen, Y., Valade, A., ... & Ghattas, J. (2015).
21 A vertically discretised canopy description for ORCHIDEE (SVN r2290) and the
22 modifications to the energy, water and carbon fluxes. *Geoscientific Model Development*, 8,
23 2035-2065.
- 24 Nightingale, P.D., et al. 2000. In situ evaluation of air-sea gas exchange parameterizations
25 using novel conservative and volatile tracers. *Glob. Biogeochem Cycles*, **14**, 373-387.
- 26 Olson, J., Watts, J.A., and Allison, L.J. (1983), Carbon in Live Vegetation of Major World
27 Ecosystems, ORNL-5862, Oak Ridge National Laboratory, Oak Ridge, Tennessee, 164pp.
- 28 Papale, D. (2006), Towards a standardized processing of Net Ecosystem Exchange measured
29 with eddy covariance technique: algorithms and uncertainty estimation, [online] Available
30 from: <http://dspace.unitus.it/handle/2067/1321> (Accessed 27 August 2013)
- 31 Parton W, Stewart J, Cole C, (1988), Dynamics of C, N, P and S in grassland soils: a model.
32 *Biogeochemistry*, **5**: 109-31.
- 33 Peylin P, Rayner PJ, Bousquet P, et al. (2005), Daily CO₂ flux estimates over Europe from
34 continuous atmospheric measurements: 1, inverse methodology, *Atmospheric Chemistry and*
35 *Physics*, **5**: 3173-3186.
- 36 Piao, S., Sitch, S., Ciais, P., Friedlingstein, P., Peylin, P., Wang, X., Ahlström, A., Anav, A.,
37 Canadell, J. G., Cong, N., Huntingford, C., Jung, M., Levis, S., Levy, P. E., Li, J., Lin, X.,

- 1 Lomas, M. R., Lu, M., Luo, Y., Ma, Y., Myneni, R. B., Poulter, B., Sun, Z., Wang, T., Viovy,
2 N., Zaehle, S. and Zeng, N.: Evaluation of terrestrial carbon cycle models for their response to
3 climate variability and to CO₂ trends, *Glob. Change Biol.*, 19(7), 2117–2132,
4 doi:10.1111/gcb.12187, 2013.
- 5 Prentice, I. C., Liang, X., Medlyn, B. E. and Wang, Y.-P.: Reliable, robust and realistic: the
6 three R's of next-generation land-surface modelling, *Atmospheric Chem. Phys.*, 15(10),
7 5987–6005, doi:10.5194/acp-15-5987-2015, 2015.
- 8 [Raoult, N. M., Jupp, T. E., Cox, P. M., and Luke, C. M.: Land surface parameter optimization](#)
9 [through data assimilation: the adJULES system, *Geosci. Model Dev. Discuss.*,](#)
10 [doi:10.5194/gmd-2015-281, in review, 2016.](#)
- 11 Rayner, P. J., Scholze, M., Knorr, W., Kaminski, T., Giering, R. and Widmann, H.: Two
12 decades of terrestrial carbon fluxes from a carbon cycle data assimilation system (CCDAS), ,
13 19, doi:10.1029/2004GB002254, 2005.
- 14 Rayner, P. J. (2010). The current state of carbon-cycle data assimilation. *Current Opinion in*
15 *Environmental Sustainability*, 2(4), 289-296.
- 16 Regnier, P., Friedlingstein, P., Ciais, P., Mackenzie, F. T., Gruber, N., Janssens, I. A., ... &
17 Arndt, S. (2013). Anthropogenic perturbation of the carbon fluxes from land to ocean. *Nature*
18 *Geoscience*, 6(8), 597-607.
- 19 Ricciuto, D. M., A. W. King, D. Dragoni, and W. M. Post (2011), Parameter and prediction
20 uncertainty in an optimized terrestrial carbon cycle model: Effects of constraining variables
21 and data record length, *J. Geophys. Res.*, 116, G01033, doi:10.1029/2010JG001400.
- 22 Ricciuto, D. M., Butler, M. P., Davis, K. J., Cook, B. D., Bakwin, P. S., Andrews, A. and
23 Teclaw, R. M.: Causes of interannual variability in ecosystem-atmosphere CO₂ exchange in a
24 northern Wisconsin forest using a Bayesian model calibration, *Agric. For. Meteorol.*, 148(2),
25 309–327, doi:10.1016/j.agrformet.2007.08.007, 2008.
- 26 Richardson, A. D., Williams, M., Hollinger, D. Y., Moore, D. J. P., Dail, D. B., Davidson, E.
27 a., Scott, N. a., Evans, R. S., Hughes, H., Lee, J. T., Rodrigues, C. and Savage, K.: Estimating
28 parameters of a forest ecosystem C model with measurements of stocks and fluxes as joint
29 constraints, *Oecologia*, 164(1), 25–40, doi:10.1007/s00442-010-1628-y, 2010.
- 30 Rivier L., Ciais P., Hauglustaine D.A., et al. (2006), Evaluation of SF₆, C₂Cl₄, and CO to
31 approximate fossil fuel CO₂ in the Northern Hemisphere using a chemistry transport
32 model, *Journal Geophysical Research-Atmosphere*, 111(D16) - D16311.
- 33 Rödenbeck, C., T. J. Conway, and R. L. Langenfelds (2006), The effect of systematic
34 measurement errors on atmospheric CO₂ inversions: A quantitative assessment, *Atmos.*
35 *Chem. Phys.*, 6, 149–161, doi:10.5194/acp-6-149-2006.
- 36 Rödenbeck C., D.C.E. Bakker, N. Gruber, Y. Iida, A. Jacobson, S. Jones, P. Landschutzer, N.
37 Metzl, S. Nakaoka, A. Olsen, G.-H. Park, P. Peylin, K.B. Rodgers, T.P. Sasse, U. Schuster,
38 J.D. Shutler, V. Valsala, R. Wanninkhof, and J. Zeng, 2015. Data-based estimates of the

1 ocean carbon sink variability – First results of the Surface Ocean pCO₂ Mapping
2 intercomparison (SOCOM). *Biogeosciences*, 12: 7251-7278. [doi:10.5194/bg-12-7251-2015](https://doi.org/10.5194/bg-12-7251-2015).

3 Rosenblatt, F. (1958). The perceptron: a probabilistic model for information storage and
4 organization in the brain. *Psychological review*, 65(6), 386.

5 Ruimy A, Dedieu G, Saugier B, (1996), TURC: A diagnostic model of continental gross
6 primary productivity and net primary productivity. *Global Biogeochemical Cycles*, **10**: 269-
7 85.

8 Sabine, C.L., et al. 2004. The oceanic sink for anthropogenic CO₂. *Science*, **305** (5682), 367-
9 371.

10 Saito, M., A. Ito and S. Maksyutov, Optimization of a prognostic biosphere model for terrestrial
11 biomass and atmospheric CO₂ variability, *Geosci. Model Dev.*, 7, 1829-1840, doi:10.5194/gmd-7-
12 1829-2014, 2014.

13 Santaren, D., Peylin, P., Bacour, C., Ciais, P. and Longdoz, B.: Ecosystem model
14 optimization using in situ flux observations: benefit of Monte Carlo versus variational
15 schemes and analyses of the year-to-year model performances, *Biogeosciences*, 11(24), 7137–
16 7158, 2014.

17 [Schurmann, G. J., Kaminski, T., Kostler, C., Carvalhais, N., Voßbeck, M., Kattge, J., Giering,](#)
18 [R., Rodenbeck, C., Heimann, M., and Zaehle, S.: Constraining a land surface model with](#)
19 [multiple observations by application of the MPI-Carbon Cycle Data Assimilation System,](#)
20 [Geosci. Model Dev. Discuss., doi:10.5194/gmd-2015-263, in review, 2016.](#)

21 Sitch, S., Friedlingstein, P., Gruber, N., Jones, S. D., Murray-Tortarolo, G., Ahlström, A.,
22 Doney, S. C., Graven, H., Heinze, C., Huntingford, C., Levis, S., Levy, P. E., Lomas, M.,
23 Poulter, B., Viovy, N., Zaehle, S., Zeng, N., Arneth, A., Bonan, G., Bopp, L., Canadell, J. G.,
24 Chevallier, F., Ciais, P., Ellis, R., Gloor, M., Peylin, P., Piao, S., Le Quéré, C., Smith, B.,
25 Zhu, Z. and Myneni, R.: Recent trends and drivers of regional sources and sinks of carbon
26 dioxide, *Biogeosciences*, 12, 653–679, doi:10.5194/bgd-12-653-2015, 2015.

27 Takahashi, et al. 2009, Corrigendum to "Climatological mean and decadal change in surface
28 ocean pCO₂, and net sea-air CO₂ flux over the global oceans" *Deep Sea Res. II*, **56**, 554-577.

29 Tarantola A. (1987), Inverse problem theory: Methods for data fitting and parameter
30 estimation. Elsevier, Amsterdam.

31 Tarantola, A. (2005), Inverse problem theory and methods for model parameters
32 estimation, *Society for Industrial and Applied Mathematics*, Philadelphia, ISBN 0-89871-572-
33 5.

34 Thum, T., MacBean, N., Peylin, P., Bacour, C., Santaren, D., Longdoz, B., Loustau, D. and
35 Ciais, P., The potential of forest biomass data in addition to carbon and water flux
36 measurements to constrain ecosystem model parameters: Case studies at two temperate forest
37 sites, *Agriculture and Forest Meteorology*, in revision, 2015.

1 Tiedtke M. (1989), A comprehensive mass flux scheme for cumulus parameterization in
2 large-scale models, *Monthly Weather Review*, **117**(8): 1779-1800

3 Tucker, C. J. (1979). Red and photographic infrared linear combinations for monitoring
4 vegetation. *Remote Sensing of Environment*, **8**, 127-150.

5 Twine, T. E., W. P. Kustas, J. M. Norman, D. R. Cook, P. R. Houser, T. P. Meyers, J. H.
6 Prueger, P. J. Starks, and M. L. Wesely (2000), Correcting eddy-covariance flux
7 underestimates over a grassland, *Agric. For. Meteorol.*, **103**(3), 279–300, doi:10.1016/S0168-
8 1923(00)00123-4.

9 Verant, S., Laval, K., Polcher, J., and De Castro, M. (2004), Sensitivity of the continental
10 hydrological cycle to the spatial resolution over the Iberian Peninsula, *Journal of*
11 *Hydrometeorology*, **5**, 267-285.

12 Vermote, E., C.O. Justice and F-M Breon (2009), Towards a generalized approach for
13 correction of the BRDF effect in MODIS directional reflectances, *IEEE Transactions on*
14 *Geoscience and Remote Sensing*, **47**, 3, 898-908.

15 Wang, Y. P., Baldocchi, D., Leuning, R., Falge, E. and Vesala, T.: Estimating parameters in a
16 land-surface model by applying nonlinear inversion to eddy covariance flux measurements
17 from eight FLUXNET sites, *Glob. Change Biol.*, **13**(3), 652–670, doi:10.1111/j.1365-
18 2486.2006.01225.x, 2007.

19 Wang, Y. P., Leuning, R., Cleugh, H. and Coppin, P.: Parameter estimation in surface
20 exchange models using nonlinear inversion : how many parameters can we estimate and
21 which measurements are most useful ?, *Glob. Change Biol.*, **7**, 495–510, doi:10.1046/j.1365-
22 2486.2001.00434.x, 2001.

23 Wanninkhof, R., 1992. Relationship between wind speed and gas exchange. *J. Geophys.*
24 *Res.* **97**, 7373-7382.

25 Weiss, R.F., 1974. Carbon dioxide in water and seawater: the solubility of a non-ideal gas.
26 *Mar. Chem.*, **2**, 203-215.

27 Welp, L. R., Keeling, R. F., Meijer, H. A., Bollenbacher, A. F., Piper, S. C., Yoshimura, K.,
28 ... & Wahlen, M. (2011). Interannual variability in the oxygen isotopes of atmospheric CO₂
29 driven by El Nino. *Nature*, **477**(7366), 579-582.

30 Williams, M., Schwarz, P. a, Law, B. E., Irvine, J. and Kurpius, M. R.: An improved analysis
31 of forest carbon dynamics using data assimilation, *Glob. Change Biol.*, **11**(1), 89–105,
32 doi:10.1111/j.1365-2486.2004.00891.x, 2005.

33 Xiao, J., Davis, K. J., Urban, N. M. and Keller, K.: Uncertainty in model parameters and
34 regional carbon fluxes: A model-data fusion approach, *Agric. For. Meteorol.*, 189-190, 175–
35 186, doi:10.1016/j.agrformet.2014.01.022, 2014.

36 [Yapo, P.O., Gupta, H.V. and Sorooshian, S., Multi-objective global optimization for](#)
37 [hydrologic models, *J. Hydrol.*, **204**, 83-97, 1998.](#)

- 1 Zobitz, J. M., D. J. P. Moore, T. Quaife, B. H. Braswell, A. Bergeson, J. A. Anthony, and R.
2 K. Monson (2014), Joint data assimilation of satellite reflectance and net ecosystem exchange
3 data constrains ecosystem carbon fluxes at a high-elevation subalpine forest, *Agric. For.*
4 *Meteorol.*, 195–196, 73–88.
- 5 Zobler, L (1986), A world soil file for global climate modeling, NASA Technical
6 Memorandum 87802. NASA Goddard Institute for Space Studies, New York, U.S.A.
- 7
- 8

1 Tables

2 Table 1. Parameters description, generality (PFT dependent, global, specific to FLUXNET
3 sites or for a set of regions) and data stream(s) that were used to constrain them.

Parameter	Description	Dependent	Constraint
V_{cmax}	Maximum carboxylation rate ($\mu\text{mol}\cdot\text{m}^{-2}\cdot\text{s}^{-1}$)	PFT	Flux, CO ₂
$G_{s,slope}$	Ball-Berry slope	PFT	Flux, CO ₂
$C_{T,opt}$	Optimal photosynthesis temperature (°C)	PFT	Flux, CO ₂
SLA	Specific leaf area ($\text{m}^2\cdot\text{g}^{-1}$)	PFT	Flux, CO ₂
$K_{LAI,happy}$	LAI threshold to stop using carbohydrate reserves	PFT	Sat, Flux, CO ₂
$K_{pheno,crit}$	Multiplicative parameter of the threshold that determines the start of the growing season	PFT	Sat, Flux, CO ₂
$L_{age,crit}$	Average critical age of leaves (days)	PFT	Sat, Flux, CO ₂
$C_{T,sen}$	Temperature threshold for senescence (°C)	PFT	Sat, Flux, CO ₂
$F_{stress,h}$	Parameter reducing the hydric limitation of photosynthesis	PFT	Flux, CO ₂
MR_{offset}	Offset of the temperature dependence of maintenance respiration	Global	Flux, CO ₂
$Q10$	Temperature dependency of heterotrophic respiration	Global	Flux, CO ₂
HR_{Hc}	Offset of the soil/litter moisture control function	Global	Flux, CO ₂
$K_{soilC,site}$	Multiplicative factor of the initial soil carbon pools	per Site	Flux
$K_{soilC,reg}$		30 regions	CO ₂
K_{albedo}	Multiplicative factor of the vegetation albedo	Global	Flux, CO ₂

4
5
6

1 Table 2. Prior information for all parameters except initial soil C pool multipliers: prior value,
2 uncertainty and range of variation for the different plant functional types (Tropical Broadleaf
3 Evergreen/Raingreen forests (TrBE / TrBR), Temperate Needle leaf / Broadleaf Evergreen
4 forests (TeNE, TeBE), Temperate Broadleaf Deciduous forest (TeBD), Boreal Needle leaf
5 Evergreen forests (BoNE), Boreal Broadleaf / Needle leaf Deciduous forests (BoBD / BoND)
6 and C3 grassland.

Parameter	Plant functional type								
	TrBE	TrBR	TeNE	TeBE	TeBD	BoNE	BoBD	BoND	NC3
V_{cmax}	65 ± 24 [35; 95]	65 ± 24 [35; 95]	35 ± 12.8 [19; 51]	45 ± 16 [25; 65]	55 ± 20 [30; 80]	35 ± 12.8 [19; 51]	45 ± 16 [25; 65]	35 ± 12.8 [19; 51]	70 ± 25.6 [38; 102]
$G_{s,slope}$	6.0 ± 2.4 [6; 12]	6.0 ± 2.4 [6; 12]	6.0 ± 2.4 [6; 12]	6.0 ± 2.4 [6; 12]	6.0 ± 2.4 [6; 12]	6.0 ± 2.4 [6; 12]	6.0 ± 2.4 [6; 12]	6.0 ± 2.4 [6; 12]	6.0 ± 2.4 [6; 12]
$C_{T,opt}$	37 ± 6.4 [29; 45]	37 ± 6.4 [29; 45]	25 ± 6.4 [17; 33]	32 ± 6.4 [24; 40]	26 ± 6.4 [18; 34]	25 ± 6.4 [17; 33]	25 ± 6.4 [17; 33]	25 ± 6.4 [17; 33]	27.25 ± 6.4 [19.25; 35.25]
SLA	0.015 ± 0.0092 [0.007; 0.03]	0.026 ± 0.0148 [0.013; 0.05]	0.009 ± 0.0064 [0.004; 0.02]	0.02 ± 0.012 [0.01; 0.04]	0.026 ± 0.0148 [0.013; 0.05]	0.009 ± 0.0064 [0.004; 0.02]	0.026 ± 0.0148 [0.013; 0.05]	0.009 ± 0.0064 [0.004; 0.02]	0.026 ± 0.0148 [0.013; 0.05]
$K_{LAI,happy}$	0.50 ± 0.14 [0.35; 0.70]	0.50 ± 0.14 [0.35; 0.70]	0.50 ± 0.14 [0.35; 0.70]	0.50 ± 0.14 [0.35; 0.70]	0.50 ± 0.14 [0.35; 0.70]	0.50 ± 0.14 [0.35; 0.70]	0.50 ± 0.14 [0.35; 0.70]	0.50 ± 0.14 [0.35; 0.70]	0.50 ± 0.14 [0.35; 0.70]
$K_{pheno,crit}$	—	1.0 ± 0.44 [0.7; 1.8]	—	—	1.0 ± 0.44 [0.7; 1.8]	—	1.0 ± 0.44 [0.7; 1.8]	1.0 ± 0.44 [0.7; 1.8]	1.0 ± 0.44 [0.7; 1.8]
$L_{age,crit}$	730 ± 192 [490; 970]	180 ± 48 [120; 240]	910 ± 240 [610; 1210]	730 ± 192 [490; 970]	180 ± 48 [120; 240]	910 ± 240 [610; 1210]	180 ± 48 [120; 240]	180 ± 48 [120; 240]	120 ± 60 [30; 180]
$C_{T,sen}$	—	—	—	—	12 ± 8 [2; 22]	—	7 ± 8 [−3; 17]	2 ± 8 [−8; 12]	−1.375 ± 8 [−11.375; 9.375]
$F_{stress,h}$	6.0 ± 3.2 [2; 10]	6.0 ± 3.2 [2; 10]	6.0 ± 3.2 [2; 10]	6.0 ± 3.2 [2; 10]	6.0 ± 3.2 [2; 10]	6.0 ± 3.2 [2; 10]	6.0 ± 3.2 [2; 10]	6.0 ± 3.2 [2; 10]	6.0 ± 3.2 [2; 10]
MR_{offset}	1.0 ± 0.6 [0.5; 2.0]								
$Q10$	1.99372 ± 0.8 [1.0; 3.0]								
HR_{Hc}	−0.29 ± 0.24 [−0.59; 0.01]								
K_{albedo}	1.0 ± 0.16 [0.8; 1.2]								

Main Figures

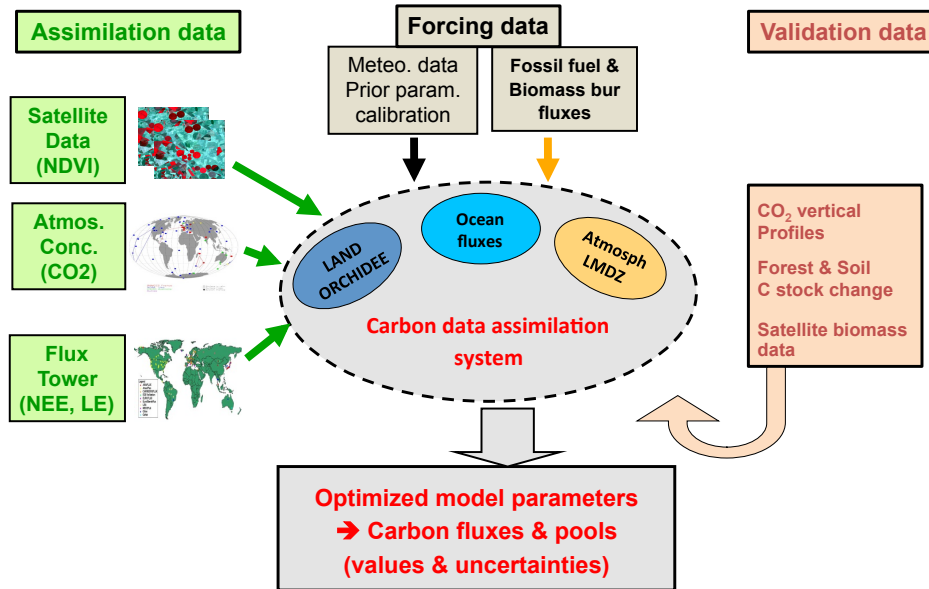


Figure 1. Schematic of the ORCHIDEE Carbon Cycle Data Assimilation System (ORCHIDAS).

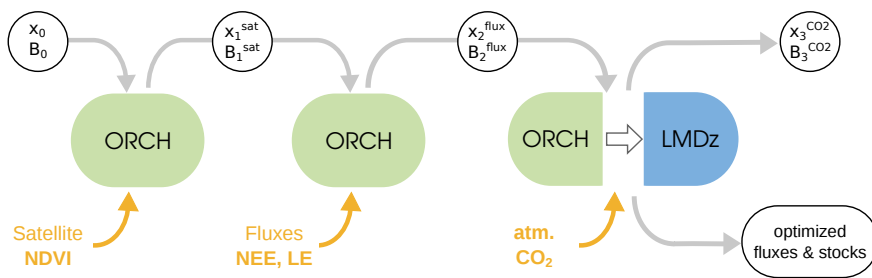


Figure 2. Illustration of the step-wise data assimilation approach used for the assimilation of multiple data streams in the ORCHIDEE-CCDAS. The list of parameters for each step is summarized in Table 1.

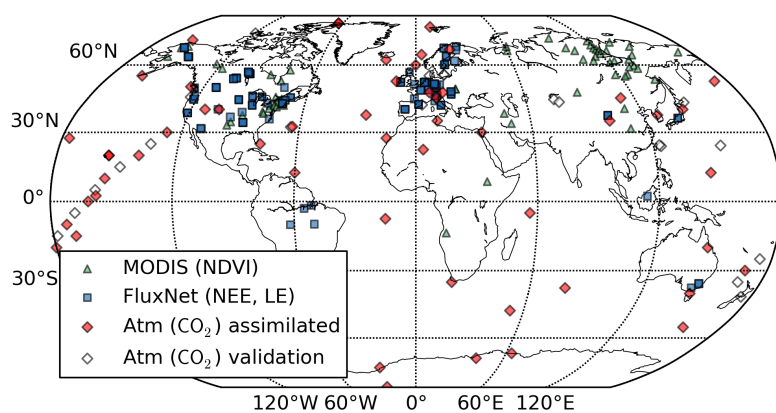


Figure 3: Location of the different observations used for each data stream assimilated in the system: MODIS-NDVI measurements, FLUXNET sites with NEE and LE measurements and atmospheric CO₂ stations (both the sites that are assimilated and the sites used for the validation).

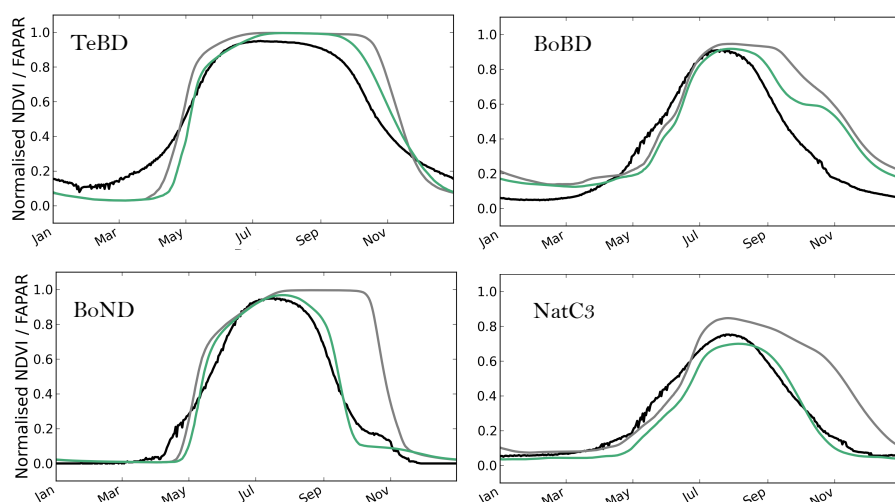


Figure 4. Mean seasonal cycle (2000-2008) of the normalised modelled FAPAR before and after optimisation, compared to that of the MODIS NDVI data, for the temperate and boreal deciduous PFTs (TeBD, BoBD, BoND and NatC3). Black = MODIS NDVI data; Grey = prior simulation (default ORCHIDEE parameters); Green = posterior multi-site optimisation.

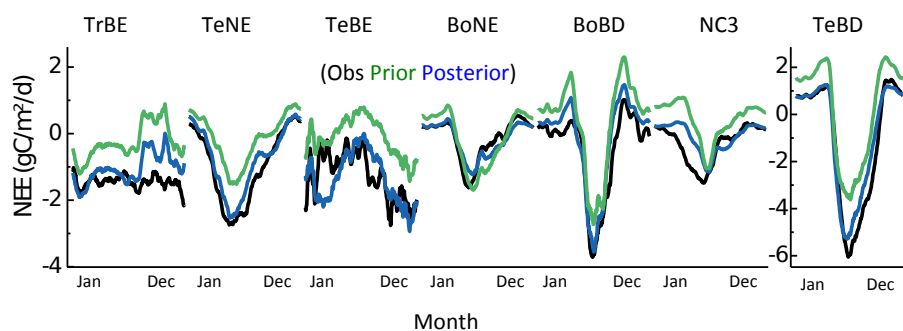


Figure 5: Mean seasonal cycle of the Net Carbon Ecosystem Exchange (NEE) for the different plant functional type optimized in Step 2 of the assimilation. The mean across all sites for a given PFT is provided for the observations (black), the posterior of step 1 (green) and the posterior of step 2 (blue).

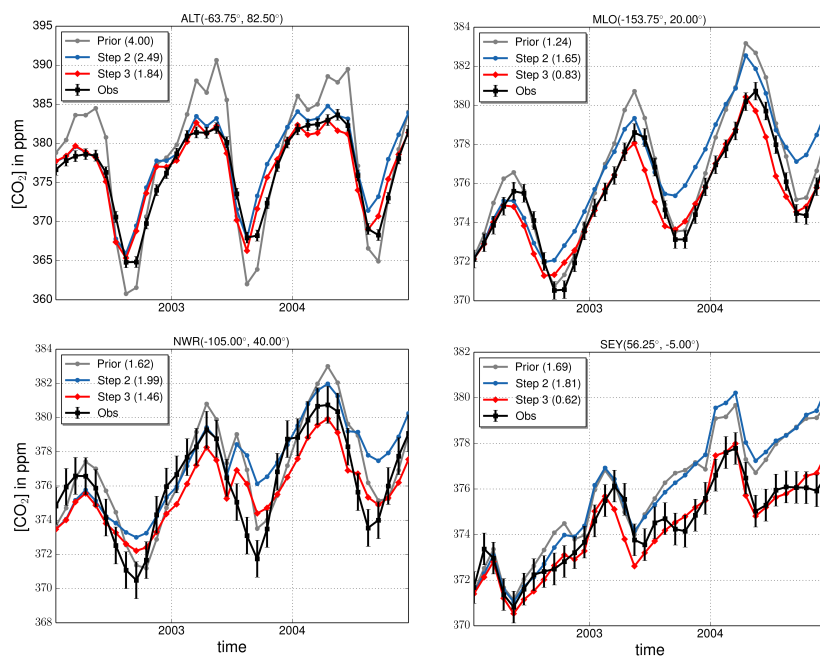
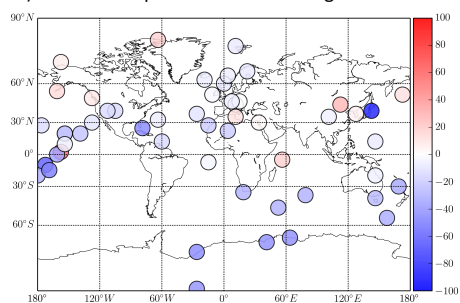
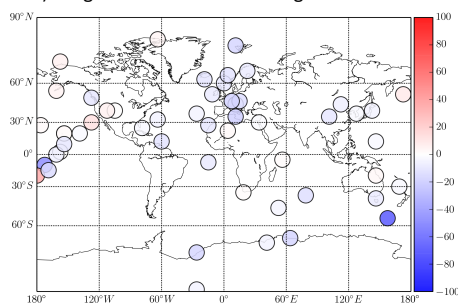


Figure 6: Monthly mean atmospheric CO₂ concentrations after step 3 of the optimization, for several stations over the period 2002-2004 of the optimization. The observations (black), the prior model (grey) and the posterior model after step 2 (blue) and step 3 (red) are displayed. Numbers in parenthesis correspond to RMSEs.

a) Seasonal amplitude: relative changes

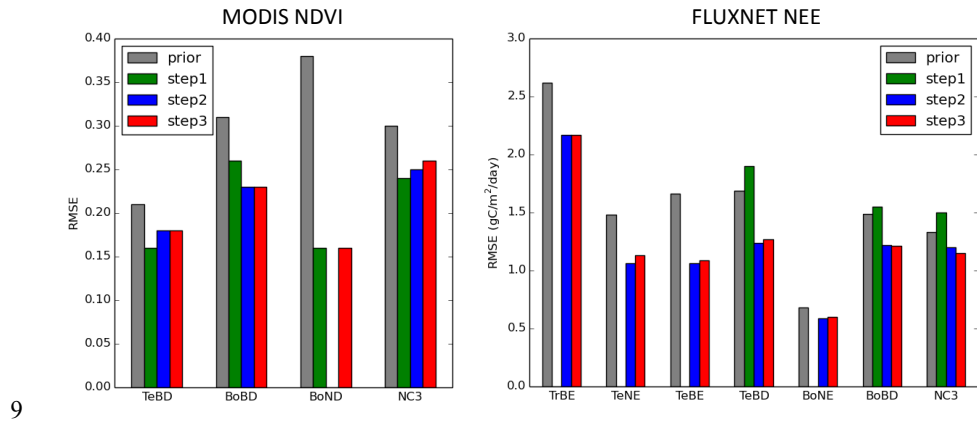


b) Length of CUP: relative changes



1 Figure 7: Changes in the mean seasonal cycle of the atmospheric CO₂ concentrations after
2 step 3 of the optimization at all atmospheric stations. Left: Relative changes (in percentage)
3 between the prior of step 3 and posterior absolute model-data differences for the amplitude of
4 the seasonal cycle. Right: Same metric but for the length of the Carbon Uptake Period (CUP),
5 measured as the sum of the days when the de-trended concentrations are negative (see text).

6
7
8



9
10 Figure 8: RMSE between model outputs and observations for two types of observations:
11 MODIS-NDVI on the left and FluxNet-NEE on the right, for different Plant Functional Types
12 (PFT: TrBE, TeNE, TeBE, TeBD, BoBD, BoND, NC3) and for the prior model simulation
13 and the posterior of each step of the assimilation framework. Missing bars correspond to the
14 fact that no data were available to constrain a given PFT.

15

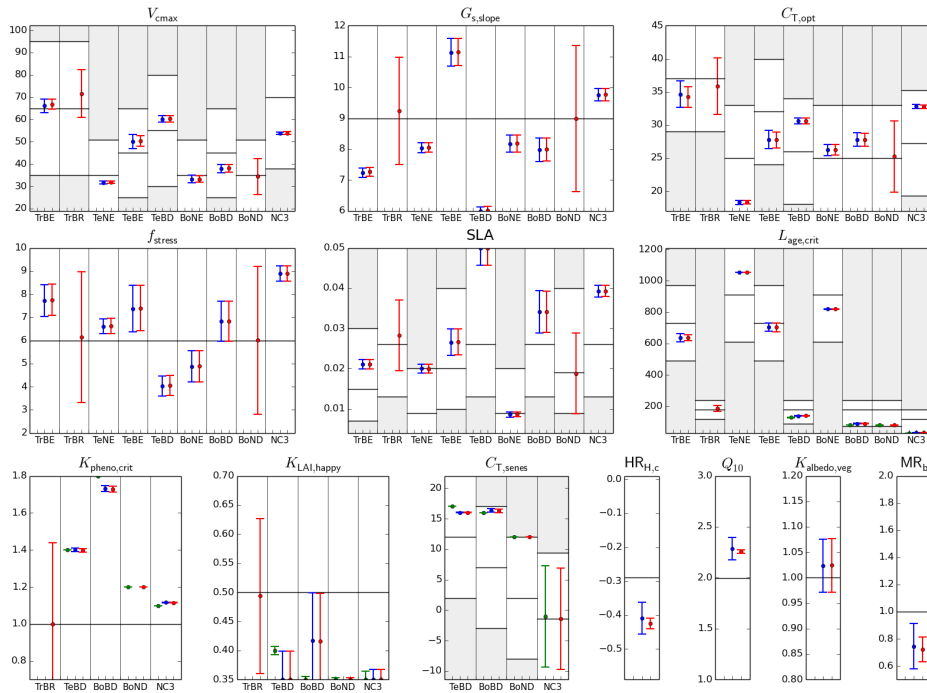
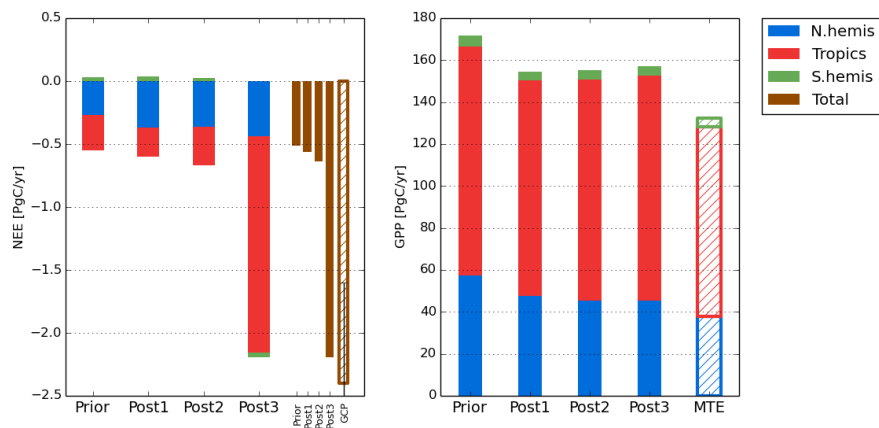


Figure 9: Prior and posterior parameter values and uncertainties for a set of optimized parameters (9 PFT dependent and 4 non-PFT dependent). The prior value corresponds to the horizontal black line and the physical allowed range of variation to the “y” range (i.e. the white zone). For PFT-dependent parameters, there are 9 sub-plots corresponding to PFTs that were optimized (except for K_{pheno_crit} with only 5 PFTs). For each parameter, there are 3 estimated values for the three successive steps: step1: assimilation of MODIS-NDVI data (green symbol); step2: adding FLUXNET data (blue symbol); step3: adding atmospheric CO₂ data (red symbol). The parameter values are depicted with the symbols and the estimated uncertainties with the vertical line (\pm sigma).



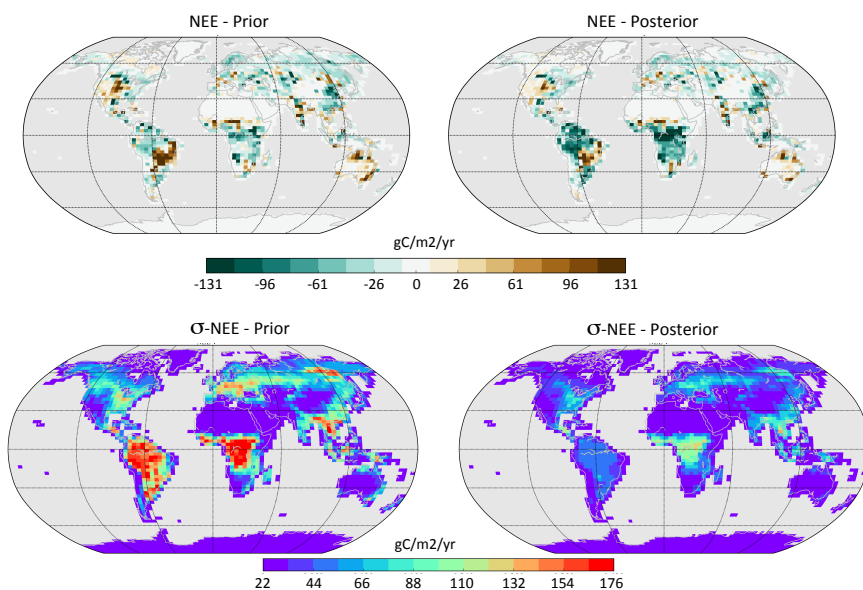
1

2 Figure 10: Left: Net Ecosystem Exchange (NEE) for three regions (North of 35°N, Tropics,
 3 South of 35°S) for the prior model, and after each step of the optimizations (mean over 2002-
 4 2004). The total NEE is indicated with the vertical brown bar and compared to the Global
 5 Carbon Project (GCP) estimate for the same period (Le Quéré et al. 2015). Right: same but
 6 for Gross Primary Production where the data driven estimate (MTE product using FluxNet
 7 data; Jung et al., 2009) is provided for comparison.

8

9

1



2

3 Figure 11: Simulated annual net carbon exchange (NEE) for the land ecosystems prior to any
 4 optimization (left column) and after step 3 of the optimization process (right column). Upper
 5 figures correspond to the mean NEE (in $\text{gC}\cdot\text{m}^{-2}\cdot\text{y}^{-1}$) over the assimilation period (2001-2003)
 6 and lower figures to the associated monthly flux uncertainties (averaged over the whole
 7 period and expressed in $\text{gC}\cdot\text{m}^{-2}\cdot\text{y}^{-1}$) due to the parameter uncertainties (see text).

8

1
2
3
4
5
6
7
8
9
10
11
12
13

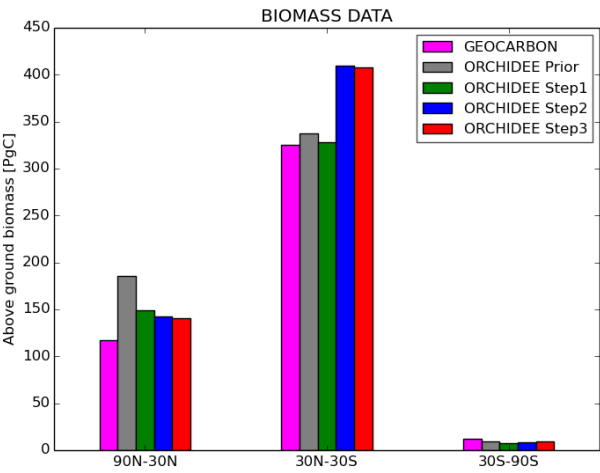


Figure 12: Above ground forest biomass data for the prior ORCHIDEE model and after step 1, step 2 and step 3 of the optimization process. Estimates from satellite observations (Santoro et al., 2015) and referred as “GEOCARBON” (following the EU-GEOCARBON project) are provided for comparison.

Appendix figures

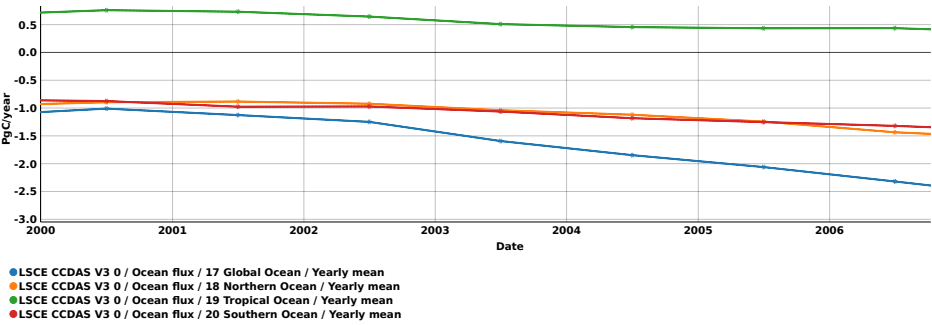
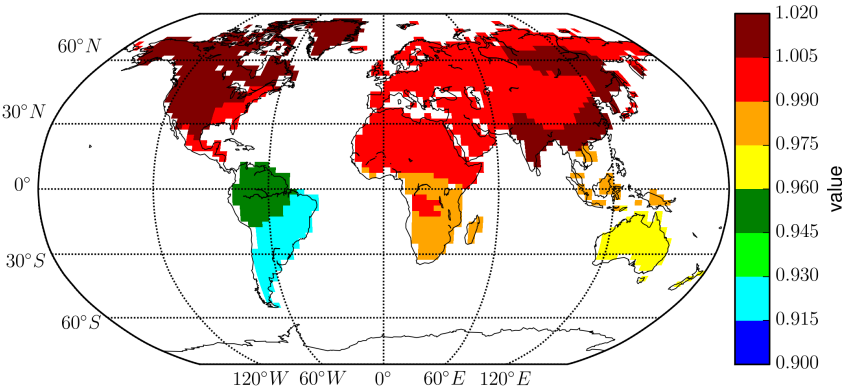


Figure A1: CO₂ air-sea fluxes including the natural ocean out-gazing, used as input to the ORCHIDEE-CCDAS and estimated from a neural network approach using observed pCO₂ data (see main text, section 2.5.1). The Northern, Tropical and Southern ocean contributions to the global ocean flux (blue curve) are also provided.

1



2

3 Figure A2: Map of the posterior values of the coefficient scaling the initial carbon pool sizes
4 per regions.

5

6